Contents lists available at ScienceDirect

Quaternary Science Reviews

Early Pleistocene invasion of Pontocaspian Fauna into the Denizli Basin (SW Anatolia): New stratigraphic constraints and implications for Aegean–Pontocaspian hydrological exchange

Sergei Lazarev [a,b,c,*], Mehmet Cihat Alçiçek [d], Lea Rausch [e,f], Marius Stoica [e], Klaudia Kuiper [g], Thomas A. Neubauer [h,i], Hemmo A. Abels [j], Thomas M. Hoyle [a,k], Christiaan G.C. van Baak [a], Anneleen Foubert [b], Diksha Bista [l], Francesca Sangiorgi [a], Frank P. Wesselingh [i,a], Wout Krijgsman [a]

[a] Department of Earth Sciences, Utrecht University, Utrecht, the Netherlands
[b] Department of Geosciences, University of Fribourg, Fribourg, Switzerland
[c] JURASSICA Museum, Porrentruy, Switzerland
[d] Department of Geology, Pamukkale University, Denizli, Turkey
[e] Department of Geology, Palaeontology and Mineralogy, Bucharest University, Bucharest, Romania
[f] PetroStrat Ltd. Tan-y-Graig, Parc Caer Seion, Conwy, Wales, United Kingdom
[g] Department of Earth Sciences, Vrije Universiteit Amsterdam, Amsterdam, the Netherlands
[h] SNSB, Bavarian State Collection for Palaeontology and Geology, Munich, Germany
[i] Naturalis Biodiversity Center, Leiden, the Netherlands
[j] Department of Geosciences and Engineering, Delft University of Technology, Delft, the Netherlands
[k] ArcStrata, Liskeard, United Kingdom
[l] British Geological Survey, Keyworth, United Kingdom

ARTICLE INFO

ABSTRACT

Aquatic biodiversity hotspots often emerge in regions with active tectonism, diverse climate conditions and complex basin configurations enabling episodic biotic isolation and exchange. The Anatolian microcontinent, located between the Mediterranean and Pontocaspian regions, has been considered a cradle of biodiversity for continental aquatic organisms. The Denizli Basin succession of SW Anatolia contains a "*Didacna*" mollusc fauna that could be the precursor of the modern Pontocaspian mollusc faunas of the Black Sea-Caspian Sea regions. However, the appearance of Pontocaspian faunas in the Denizli Basin and constraints upon their ages and dispersal pathways remain enigmatic. Moreover, the emergence of the Pontocaspian biota far into the Anatolian continental interior raises questions regarding the connectivity history and tectonic evolution of the Anatolian, Aegean and Pontocaspian realms. Here, we present an integrated stratigraphy of the ~1 km thick succession of the Kolankaya Formation of the Denizli Basin, previously assigned to the Late Miocene. To date the first occurrence of Pontocaspian fauna in the Denizli Basin and to characterise accompanying palaeoenvironmental/ palaeohydrological changes, we focus on three sets of approaches: dating (magnetostratigraphy and $^{40}Ar/^{39}Ar$), biotic record (molluscs, ostracods and dinoflagellates) and hydrological connectivity (O- and C-isotopes and $^{87}Sr/^{86}Sr$). We date the studied section as Early Pleistocene, spanning a time range of 2.6 Ma to 0.7 Ma. During that time, the Denizli Basin hosted an isolated to partially hydrologically open oligo-to mesohaline lake. The biotic record shows a drastic turnover of mollusc fauna from endemic Aegean-Anatolian and Pannonian/Paratethyan to Pontocaspian affinity at ~1.8 Ma. The palaeogeographic evolution of the region, along with the geographically limited appearance of the Pontocaspian faunas, suggests a dispersal pathway from the Black Sea Basin via the Aegean Basin. Subsequently, a short incursion into the Denizli Basin may have occurred via a series of graben-type basins: either via the Söke-Milet Basin – Büyük Menderes Graben or via Izmir Bay – Gediz Graben. Our study shows that the Denizli Basin was not a cradle but rather a sink of the Pontocaspian biota during the Early Pleistocene. The new Early Pleistocene age assignment for the Pontocaspian fauna and the Kolankaya

---

Formation in Denizli calls for a major reappraisal of models for the tectonic and stratigraphic evolution of SW Anatolia, including the regional interbasinal connectivity history.

1. Introduction

Southwestern Anatolia (Türkiye) is a continental aquatic biodiversity hotspot with both Aegean-Anatolian and Pontocaspian aquatic faunal elements (Wilke et al., 2007; Wesselingh et al., 2008; Büyükmeriç and Wesselingh, 2018; Sands et al., 2019; Rausch et al., 2020). The origin of these faunas is not well understood. The Denizli Basin, within southwestern Anatolia, contains a succession (assumed to be Late Miocene – Pliocene in age) hosting endemic faunas (ostracods and molluscs) with Parathethyan and Pontocaspian affinities (Wesselingh et al., 2008; Alçiçek et al., 2015; Rausch et al., 2020). These faunas reveal a close relationship with Neogene Parathethyan groups as well as modern endemic groups of the Caspian and the Black Sea region (the Pontocaspian region). Their presence in the Denizli Basin, therefore, raises questions about the role of Anatolia in the evolution of these biota. However, the biogeographic significance of the Denizli fauna remains unclear due to the paucity of stratigraphic age constraints.

The Denizli Basin is located in the Aegean-west Anatolian region, which is today bordered by two vast water realms – the Mediterranean to the south and southwest and the Pontocaspian region to the north and northeast (Fig. 1). The unique location within the Anatolian biodiversity hotspot and in between major biogeographic realms along with well exposed, fossiliferous basin fill make the Denizli Basin an ideal candidate to study its role in the evolution of aquatic biota in the Eurasian realm.

The Mio-Pleistocene sedimentary succession of the Denizli Basin is subdivided into four formations with rough age constraints derived from regional, small mammal faunas (Fig. 1) (Yalçınlar, 1983; Saraç, 2003; Alçiçek, 2010). The well-exposed 3D basin architecture and the aquatic and terrestrial fossil assemblages represent an excellent but underexplored archive of the region's palaeoenvironmental evolution.

In this paper, we study a ~1 km-thick section of the Kolankaya
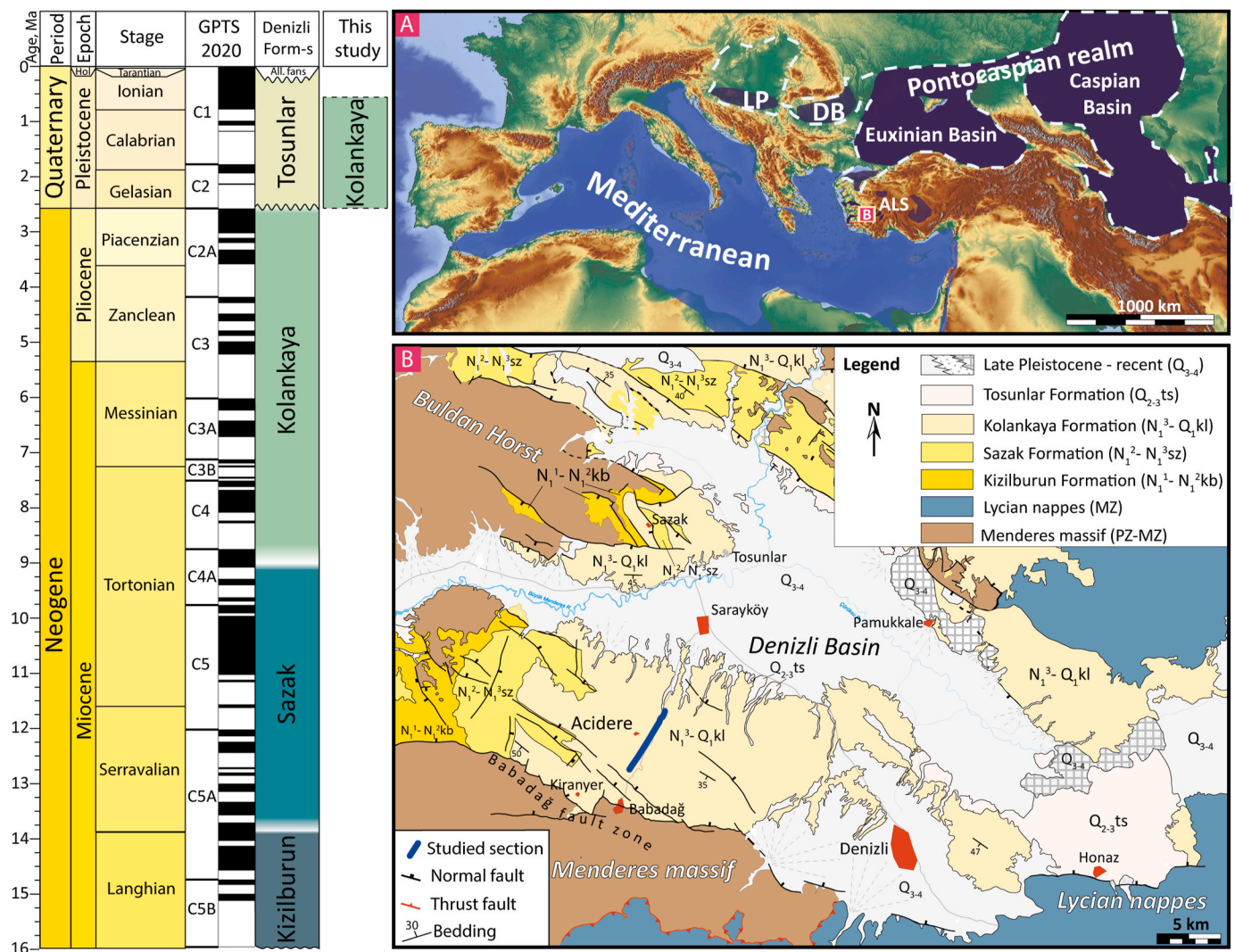
Fig. 1. Geographic overview and regional lithostratigraphic formations of the Denizli Basin (Yalçınlar, 1983; Saraç, 2003; Kaymakci, 2006; Doğan et al., 2020) correlated to the Geological Time Scale (Raffi et al., 2020). Location of the studied section: A. In the former Parathethyan realm (white dashed line) and in the Pontocaspian realm (united Caspian and Black Sea Basins), LP = Lake Pannon; ALS = Anatolian Lake System; DB – Dacian Basin. (The palaeogeographic basin configuration (light blue and dark blue) is based on Popov (2004) for the Early Pleistocene); B. In the Denizli Basin. Regional time scale and geological map are modified after Sun (1990).

Formation (Fig. 2). The integration of palaeomagnetism and ^{40}Ar/^{39}Ar dating with mollusc and ostracod fossil records enabled the tracing of a significant ecological turnover in the basin and firmly placed it within a well-defined age framework. We also combine geochemical proxies (δ^{18}O and δ^{13}C and ^{87}Sr/^{86}Sr) with sedimentary and palaeoecological observations to reconstruct successive palaeoenvironments and to further investigate whether the biotic changes in the section were linked to the changes in basin palaeohydrology. The overall aim is to date the occurrence of Pontocaspian-type faunas in the Denizli Basin and to evaluate the role of the basin in the evolution of these biotas.

2. Geological background and palaeogeographic setting

SW Anatolia belongs to the Aegean-west Anatolian extensional province whose structural evolution is determined by two major plate tectonic processes: (I) roll-back of the Aegean slab initiated in the latest Oligocene and resulting from subduction of the African plate underneath the Eurasian plate (Le Pichon et al., 1982; Gautier et al., 1999) and (II) westward escape of the Anatolian Block along the North and East Anatolian Fault Zones initiated in the Late Miocene (Şengör and Yilmaz, 1981). Starting from the Late Miocene, SW Anatolia experienced an extensional phase characterised by amplified exhumation of the dome-shaped Menderes Massif and the formation of numerous NE-SW- and NW-SE-trending graben-type basins (Ten Veen et al., 2009). By the late Pliocene, many of these basins formed a semi-connected Anatolian Lake System that collapsed during the Early Pleistocene (Alçiçek et al., 2019). The numerous graben-type basins of this former lacustrine system have been extensively studied (Alçiçek, 2010; Alçiçek and Jiménez-Moreno, 2013; Alçiçek et al., 2019), but mostly lack solid age constraints, which extremely complicates an overall understanding of the regional palaeogeographic evolution.

The Denizli Basin, 70 km long and 50 km wide, is one of these ESE-trending graben-type basins of SW Anatolia (Fig. 1). The Babadağ fault zone bounds the southern margin of the basin. The western part of the basin is divided by the Buldan horst into two segments: 1. the northern segment bounded by SE-trending normal faults and extending north-westwards into the Alaşehir (Gediz) Basin; 2. The southern segment is confined by and extends into the Büyük Menderes Basin to the west (Fig. 1) (Alçiçek et al., 2007). The sedimentary infill of the Denizli Basin has been subdivided into four lithological formations (Fig. 1) (Sun, 1990). The lower part is formed by the Langhian Kızılburun Formation, which is built of alluvial-fan deposits with conglomerates, sandstones and mudstones and comprises an MN6 micromammal assemblage (Erten et al., 2014). The following early Serravalian–early Tortonian Sazak Formation, conformably overlying the Kızılburun Formation, is made of shallowing upwards lacustrine deposits with marlstones, limestones and gypsarenites and contains an MN6–8 micromammal assemblage (Saraç, 2003). Next, the late Tortonian–Piacenzian Kolankaya Formation (but see age reappraisal below) comprises alternating marlstones, siltstones and claystone. In its upper parts, sandstones and conglomerates are more common (Alçiçek et al., 2015). Mammalian faunas from the lower part of the Kolankaya Formation are attributed to MN11–12 (Sickenberg and Tobien, 1971; Yalçınlar, 1983; Saraç, 2003; Doğan et al., 2020). The Pleistocene Tosunlar Formation unconformably overlies the Kolankaya Formation and is composed of yellowish-brownish sandstone, siltstones, conglomerates, mudstone and clayey limestone (Alçiçek et al., 2015). A micromammal fauna from the Tosunlar locality was assigned to MN17 (Kaymakci, 2006).

The Miocene to Pleistocene palaeogeography and hydrological connectivity of SW Anatolia with the Mediterranean and Paratethys (and its successor Pontocaspian realm) is uncertain due to the lack of well-dated post-Messinian outcrops in the Aegean region (Krijgsman et al., 2020a). The scarce data from mollusc faunas of Greece and Türkiye show that the marginal subbasins of the Aegean contain mixed Aegean-Anatolian mollusc fauna with Parathethyan/Pontocaspian elements (Gramann and Kockel, 1969; Koskeridou and Ioakin, 2009; Esu and Girotti, 2015;

Krijgsman et al., 2020b). The Pontocaspian region itself underwent a major palaeoecological reorganisation in the Early Pleistocene. The establishment of a hydrological connection between the Black Sea and Caspian Sea basins at 2.1 Ma led to an invasion of Pontocaspian faunal groups (molluscs, ostracods, foraminifera etc.) in the Caspian Sea Basin, forming the Pontocaspian biogeographic realm that has persisted in the region until today (Krijgsman et al., 2019; Lazarev et al., 2019). In this context, improved age data for the Denizli succession are required to understand its role in the biogeographic evolution of the Pontocaspian domain.

3. Material & methods

3.1. Section and logging

Our study concerns a 937-m-long section within the Kolankaya Formation (Fig. 2). The composite section is located in the south-western part of the Denizli Basin along the Babadağ–Sarayköy road, in the vicinity of the Acidere village (Figs. 1 and 2). The section trends perpendicular to the SW basin margin that is delimited by the active WNW-trending Babadağ fault zone. The stratigraphic thickness was measured using a Jacob's staff and calculated (for non-exposed intervals) using the parameters of bedding orientation, the distance between GPS points and their altitude. GPS coordinates of the transect bases are available in Supplementary 1.

3.2. Magnetostratigraphy

For magnetostratigraphic and rock magnetic property analyses, 241 standard cylindrical doublet samples were taken using a portable battery drill equipped with a diamond crone and a water pump. For each core, sample azimuth and inclination were measured, and a local declination correction of 5° was added (September 2015, https://www.ngdc.noaa.gov). All palaeomagnetic measurements were performed at the Palaeomagnetic laboratory "Fort Hoofddijk" (Utrecht, the Netherlands) and followed the methodology of Lazarev et al. (2019).

Out of 241 samples, 212 samples were stepwise thermally demagnetised with increments of 30–40 °C and 29 samples were demagnetised in alternating field (af) with increments of 5–10 mT, both in zero field conditions. Interpretation of results, including determination of polarity and statistical analyses, was conducted using the online platform Palaeomagnetism.org (Koymans et al., 2016). The initial file with the data is available as Supplementary 2. For the correlation of magnetic polarity patterns, we used the Geomagnetic Polarity Time Scale (GPTS) 2020 (Raffi et al., 2020).

3.3. ^{40}Ar/^{39}Ar dating

One volcanic tephra layer was identified in the studied outcrop at 114 m (GPS 37 50,3160 N, 28 52,3170 E). We sampled the top and base of this ash layer (Samples DBA-1a and 1b, Supplementary 3). Feldspar and biotite from these samples were separated using standard mineral separation procedures and were measured at the Vrije Universiteit Amsterdam on an Argus VI + noble gas mass spectrometer. Ages are calculated with decay constants of Min et al. (2000) and an age of 28.201 Ma for Fish Canyon sanidine (Kuiper et al., 2008). The atmospheric ^{40}Ar/^{36}Ar air value of 298.56 is used (Lee et al., 2006). All errors are quoted at the 2σ level. Analytical procedures and relevant analytical data are reported in Supplementary 3.

3.4. Mollusc palaeontology

Mollusc occurrences were documented in the sections, together with taphonomic characterisation (sorting, abrasion, occurrence of incompatible ecological taxa). The faunas from the upper part of the section have been extensively described before (Wesselingh et al., 2008; Alçiçek
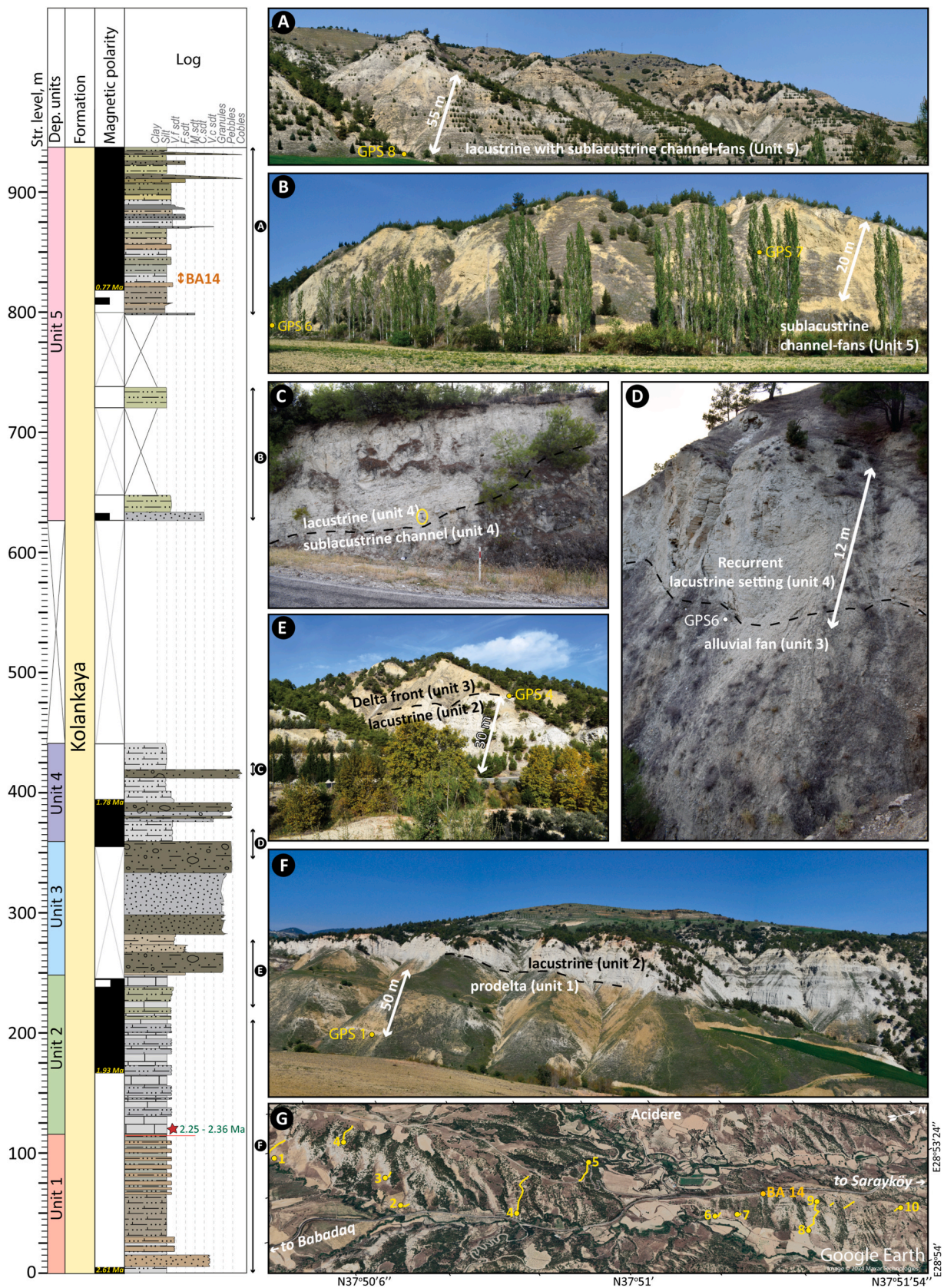
Fig. 2. Composite log with five depositional units and their representative pictures. A–F: pictures of outcrops indicated on the log; G. Satellite map of the studied area with indicated GPS points and logging paths (yellow lines) and BA14 mollusc locality of Wesselingh et al. (2008). GPS coordinates are available in Supplementary 1. Magnetic polarity patterns and ages are presented in chapters 4.2.1 and 5.1.

et al., 2015) and identification of species in the field was straightforward. For the lower parts of the section, faunas were observed in the interval 100–250 m and two shelly levels (200 m and 230 m) were sampled to assess the species composition and their ecological and biogeographic signature. The sample from the 200 m level is from a coarse-grained sand interval and consists of a combination of larger gastropod specimens picked from the surface and a small amount of fossiliferous sediment, washed over 0.5 mm. The sample from the 230 m level contained about 3 kg of shell-bearing silts that were washed and sieved over 0.5 mm. The taxonomy of the fauna has been reported by Neubauer and Wesselingh (2023).

3.5. Ostracod palaeontology

The ostracod data from the studied outcrop have been published in Rausch et al. (2020), where their 185-thick section B corresponds to the interval of 797.5–837 m in our composite outcrop (thickness difference is caused by lateral changes of conglomerates in the upper part of the section) and their 90-m-thick section A – to the interval 186–276 m. For ostracods, 21 micropalaeontological samples were analysed from Unit 2 and 62 from Unit 5. Samples from Unit 4 contained a poorly preserved ostracod assemblage and were not included in this study. All micropalaeontological samples were recovered from fine-grained sediments (clayey siltstones and sandy limestones) and processed using standard micropalaeonontological methods. In this manuscript, we revised these data according to the updated age constraints.

3.6. Palynological analyses and dinoflagellate cysts as environmental indicators

Sixteen samples were qualitatively analysed for dinoflagellate cysts (dinocysts) and other palynomorphs (pollen, freshwater and brackish-water algae and acritarches). Samples were processed at Utrecht University using cold HCl (30 %) to remove carbonates and cold HF (38 %) to dissolve silicates. Samples were ultrasonicated (5 min) and subsequently sieved through meshes (125 and 10 μm). The residues (10–125 μm fraction) were mounted on slides using glycerine jelly and sealed with lacquer. Slides were scanned for palynomorphs in order to detect fossils indicative of depositional environments. Identifications were made using several reference texts (Wall et al., 1973; Sütő-Szentai, 1982, 2010; Sütő-Szentai, 2000; Mudie et al., 2001, 2017; Rochon et al., 2002; Marret and Zonneveld, 2003; Shumilovskikh et al., 2013; Zonneveld et al., 2013; Soliman and Riding, 2017).

3.7. Strontium isotope geochemistry

Six samples taken throughout the outcrop were measured for strontium isotopic ratios (^{87}Sr/^{86}Sr) (Supplementary 1). For each sample, 3–5 unaltered ostracod valves were used. Sample preparation and analysis were carried out using the method described by Bista et al. (2021) and were performed on a Thermo-Finnegan Triton thermal ionisation mass spectrometer (TIMS) at the University of Bristol. The Instrument performance was monitored using the NBS987 Sr standard, which produced an average of 0.710247 ± 0.000005 (2 SD, n = 81) throughout the study. Procedural Sr blank was negligible based on replicate measurement of NBS987 Sr with each batch of column chromatography (0.710248 ± 0.000006, n = 41).

3.8. Stable O and C isotopes

Stable isotopes of oxygen and carbon on bulk sediment were measured on 63 samples spanning the section using a Thermo Finnigan GasBench II equipped with a CTC Combi-Pal autosampler and linked to Finnigan MAT 252 mass spectrometer at the University of Lausanne following the methodology of Spötl and Vennemann (2003). The stratigraphic levels and all O and C values can be found in Supplementary 1.

4. Results

4.1. Section and logging

The studied outcrop was subdivided into five depositional units based on genetically-related sedimentary facies (Fig. 2). The lowermost Unit 1 (0–115 m) is composed of alternating brown and greenish-grey medium-bedded (beds of 5–10 cm) siltstones and occasional fine-grained sandstones and marlstones (Fig. 2F). At 114 m, a 12-cm thick dark purple-grey medium-grained volcanic tephra layer is present (See 4.2.2). Unit 2 (115–247 m) follows with a sharp conformable contact and is built of white to pale grey horizontally laminated to massive marlstones and limestones alternating in 1 to 7-m-thick beds (Fig. 2F). Unit 3 (247–358 m) covers Unit 2 with a 2-m-thick basal horizon of intraformational breccia built of reworked marlstone clasts (Fig. 2D). Unit 3 consists of vertically and laterally extensive (up to 30 m-thick) packages of fine-to very coarse-grained sandstones with frequent, up-to 7 m-thick, conglomerates. Unit 4 (358–441 m) is characterised by a return of white to pale grey marlstones, similar to those in Unit 2, with occasional laterally-confined incisions filled with alternating coarse-grained sandstones and conglomerates (Fig. 2C–E). The 358–626 m interval lacks exposure, but given the morphology and the scree, it is likely a fine-grained interval. Unit 5 (626–936.8 m) is dominated by an alternation of brown, marly siltstones and white marlstones in the lower part and interrupted by channelised conglomerate-filled incisions up to 40-m thick to the top part (Fig. 2A and B).
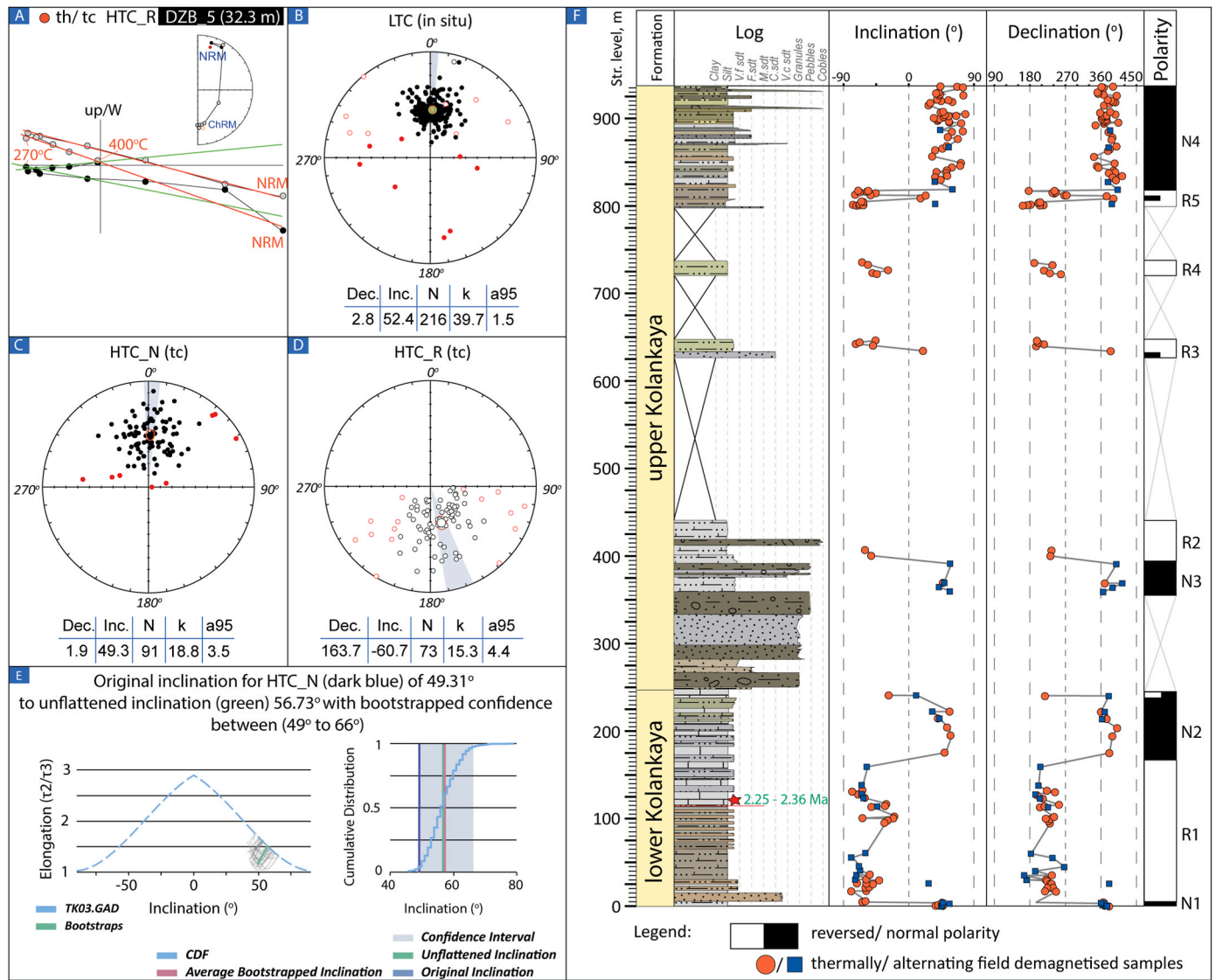
4.2. Dating

4.2.1. Magnetostratigraphy

The thermal demagnetisation of 238 samples from the Denizli section revealed two magnetic components. The first is a low-temperature component (LTC) that demagnetises up to 270 °C (in some samples up to 360 °C) or up to 25 mT and has only normal polarity directions (Fig. 3A). The LTC is a dominant component in all studied samples and on average contributes to 80 % of the total Natural Remanent Magnetisation. The average direction of the LTC component is: D = 2.75°, I = 52.44°, k = 39.65, α95 = 1.54 for N = 216 in geographic coordinates (Fig. 3B). These inclination values are very close to the expected inclination for the present-day magnetic field in Denizli of 55° (https://www.ngdc.noaa.gov, on March 2016). We thus interpret the LTC as representing a secondary viscous magnetic overprint by the present-day field.

The second, high-temperature (HTC) component fully demagnetises in a temperature range of 300–400 °C or between 25 and 100 mT, trends towards the origin of the Z-plot and shows both, normal (HTC_N) and reversed (HTC_R) directions (Fig. 3A). The mean direction for normal polarity samples has parameters of D = 1.93°, I = 49.31°, k = 18.82, α95 = 3.47 for N = 93 samples in tectonically corrected coordinates (tc) (Fig. 3C), while for reversed samples D = 163.7°, I = −60.74°, k = 15.3, α95 = 4.39 for N = 73 (Fig. 3D).

The mean inclination value of the HTC_N group is about 11° shallower than those in the antipodal HTC_R reversed group. Consequently, the reversal test of McFadden and McElhinny (1990) applied to the HTC directions is negative due to the lower inclination values of the normal polarity samples. To test for a potential inclination shallowing, we applied the elongation/inclination method (E/I) that corrects for flattening using the TK03.GAD Field Model (Tauxe and Kent, 2004). The bootstrap test used in the E/I method shows an unflattened mean inclination of 56.73° for the HTC_N group (Fig. 3E). Applying this method to the reversed directions (HTC_R) did not find intersections with the TK03. Nevertheless, considering the clear statistical distinction between normal and reversed HTC components, we interpret the HTC component as primary and characteristic for the sedimentation age.

Plotting the HTC directions against stratigraphic levels results in 5 reversed polarity and 4 normal polarity zones (Fig. 3F). The section begins with a small normal zone N1 (0–3.6 m) followed by a continuous

Fig. 3. Summary of palaeomagnetic dating of the studied outcrop. A. Zijderveld diagram for a sample with representative LTC (0–270 °C) and HTC_R components (300–400°). Equal area plots for: B. LTC in geographic coordinates (in situ). Area plots of HTC in tectonic coordinates: C. normal polarity (HTC_N); D. reversed polarity (HTC_R); E. Diagram of the bootstrap test used in the Elongation/Inclination method for determination of inclination shallowing of HTC_N; F. Magnetostratigraphy of the studied outcrop. The green star indicates the stratigraphic position of the $^{40}Ar/^{39}Ar$ age of the volcanic tephra. Abbreviations: th - thermally demagnetised; tc - tectonically corrected coordinates; in situ - geographic coordinates; NRM - natural remanent magnetisation; ChRM - characteristic remanent magnetisation; Dec. - declination; Inc. - inclination; N - number of samples; k - precision parameter of Fisher (1953) a95 - 95 % cone of confidence.

reversed zone R1 (3.6–156.5 m) and after, by a normal zone N2 (156.5–240.5 m) with a single reversed sample at 240.5 m. Above the N2 lies the coarse-grained sedimentary Unit 3 that separates the lower and upper parts of the Kolankaya Formation and was not sampled for palaeomagnetism. Above Unit 3, the palaeomagnetic record continues with a normal zone N3 (359–395.4 m) followed by a reversed zone R2 (395.4–440 m). Between 440 m and 798 m, the outcrop, although badly exposed, comprises two short, reversed zones R3 (634–646 m) with a single normal polarity sample at 634 m and R4 (721.8–735.4 m). The upper part of the section consists of one short, reversed zone (R5, 800.5–818 m) succeeded by a long normal zone N4 (818–937 m).

4.2.2. $^{40}Ar/^{39}Ar$ geochronology

Two samples with 4 mineral fractions from the tephra layer in Unit 2 show a large spread in ages: sanidine (L1) and biotite (L2) from the top of the ash layer range 2.1–36.9 Ma and 1.9–28.6 Ma, respectively, while sanidine (L3) and biotite (L4) from the base of the ash layers range 2.1–12.5 Ma and 0.9–5.2 Ma, respectively. Although most (122 out of

156) of the data points plot between 2 and 3 Ma (Fig. 4). Samples are also characterised by relatively low radiogenic ^{40}Ar yields. $^{40}Ar*$ yields range 19–91% for L1-sanidine, 7–66% for L2-biotite, 18– >100% for L3-sanidine and 13–57% for L4-biotite. Low radiogenic $^{40}Ar*$ yields suggest
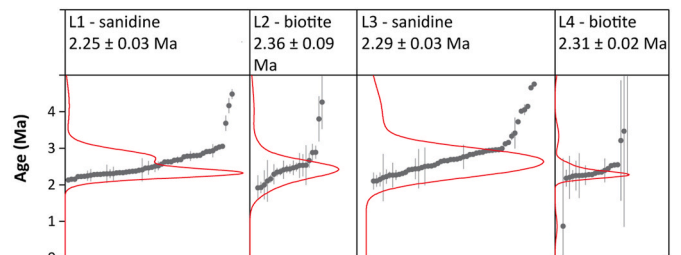
Fig. 4. Summary of $^{40}Ar/^{39}Ar$ ages of the volcanic tephra layer at 144 m in the studied outcrop. Individual analyses with their 2σ analytical uncertainty plotted in the range 0–5 Ma.

some alteration and, thus, minor Ar loss, leading to an underestimation of the age. However, we do not observe a correlation between $^{40}Ar^*$ and ages. If we focus on the data between 2 and 3 Ma, it is difficult to obtain an eruption age for this volcanic ash since we observe a continuous dataset with no clear age peak. We used the weighted mean age of the youngest sample population and included data points as long as MSWD < t-test at 95% confidence. This approach yielded 2.25 ± 0.03 Ma for L1-sanidine, 2.36 ± 0.09 Ma for L2-biotite, 2.29 ± 0.03 Ma for L3-sanidine, and 2.31 ± 0.02 Ma for L4-biotite. It is difficult to report an accurate eruption age based on these data, but we infer a depositional age between 2.25 and 2.36 Ma.

4.3. Biotic record

4.3.1. Mollusc palaeontology

The fauna from Unit 2 (115–247 m) contains at least 27 species: two species of dreissenid bivalves (*Dreissena*), two species of neritids (*Theodoxus*), one melanopsid (*Esperiana*), 16 species of hydrobiids belonging to several different subfamilies (Caspiinae: *Graecoanatolica, Iraklimelania*; Hydrobiinae: *Ecrobia, Harzhauseria*; Pyrgulinae: *Falsipyrgula, Laevicaspia, Prososthenia, Staja, Xestopyrguloides*), four species of valvatids (*Valvata*) and two lymnaeids (*Corymbina, Radix*) (Fig. 5) (Neubauer and Wesselingh, 2023). A third of the species are endemic to the Denizli Basin. About 45% have an Aegean-Anatolian character, with many of the recovered genera being typical for/or endemic to this region. Especially with Pliocene–Early Pleistocene faunas of Rhodes, Kos and mainland Greece, as well as the Çameli and Eşen Basin in Turkey, biogeographic affinities were noted (Neubauer and Wesselingh, 2023). Additionally, the general composition containing the subfamilies Caspiinae and Pyrgulinae, as well as the genera *Dreissena, Theodoxus, Ecrobia,* and *Laevicaspia*, has a clear Pontocaspian signature.

The fauna is entirely composed of aquatic species but (almost) lacks common freshwater groups such as planorbid snails, pearly freshwater mussels and sphaeriid clams. The two *Dreissena* [*D. kairanderensis, Dreissena. sp. 1*] and two *Theodoxus* [*T. percarinatus, T.* aff. *pilidei*] species that are common in the Unit 2 faunas imply the presence of hard substrate, whereas the hydrobiids likely represent soft aquatic bottoms. The dominance of hydrobiids, the frequency of strongly ornamented species in several groups, the lack of common freshwater groups and the relatively high species numbers all point to a long-lived lake with slightly elevated (possibly oligohaline) salinities during the deposition of Unit 2 fauna.

The mollusc faunas from units 4 and 5 are entirely different from those of Unit 2 (Fig. 5). The fauna is dominated by Pontocaspian taxa, such as *Didacna* species. This type of fauna was described by Wesselingh et al. (2008) from the Babadağ BA14 outcrop (correlated to 825–830 m of the studied section) and by Alçiçek et al. (2015) from the Tosunlar outcrop in the northern Denizli Basin. The BA14 fauna consists of four species of *Didacna*, one *Theodoxus* species, four hydrobiid species (the abundant and highly variable "*Micromelania" phrygica*, rare *Graecoanatolica, Pyrgula,* and ?*Pseudamnicola*), and the unusually ribbed *Valvata cincta* (=? *V. klemmi*, which still lives in the region). Within the fauna, low amounts of differentially preserved and reworked freshwater species occur, including *Radix* cf. *ampla, Sphaerium* sp. and *Pisidium* cf. *crassissimum*. The Tosunlar fauna reported by Alçiçek et al. (2015) is likely younger than that of the studied outcrop and only contains a single *Didacna* species apart from abundant *Theodoxus* and "*Micromelania*". Furthermore, the reworked freshwater component contains *Esperiana* cf. *esperi*. The mollusc fauna from Units 4 and 5 represents mesohaline lake associations with comparably low diversity (11 species) but a very high degree of endemism.

4.3.2. Ostracods

Ostracods were investigated from Unit 2 and Unit 5 contain 32 species belonging to a total of 13 genera (Fig. 6). The ostracod fauna from Unit 3 could not be obtained due to the coarse-grained lithology,

while microfauna from Unit 4 was very badly preserved and highly fragmented complicating identification. The ostracod assemblage in Unit 2 is dominated by leptocytherids, including common occurrences of *Leptocythere* sp. 1, *Amnicythere multituberculata, Amnicythere striatocostata, Amnicythere* aff. *striatocostata, Amnicythere* sp. 3, *Amnicythere* sp. 4, loxoconchid species as *Loxoconcha babazananica, Loxoconchissa (Loxocaspia)* aff. *reticulata*) as well as some rare occurrences of *Cyprideis pannonica, Amnicythere* sp. 1 and *Tyrrhenocythere* aff. *pontica*. Candonid ostracods are represented by common occurrences of *Caspiocypris carica, Typhlocyprella* sp. together with *Typhlocypris fossulata fossulata* and *Typhlocypris fossulata reticulata*. There are only minor shifts in the faunal composition, indicating the presence of a stable, brackish (oligohaline to lower mesohaline) water environment. The presence of both adults and different juvenile stages, prove the in situ character of the fauna, excluding the presence of reworking processes.

Within Unit 5 important changes in the faunal composition could be observed (Fig. 6). The ostracod community is dominated by candonids such as *Candona angulata, C.* ex. gr. *angulata* and loxoconchids as *Loxoconcha muelleri* and *L. eichwaldi* suggesting oligohaline – mesohaline conditions. In some levels, the occurrence of heavily calcified ostracod valves, accompanied by a minor diversification of the assemblage, indicates a slight increase in alkalinity. These levels contain *Amnicythere* sp. 2, *Cyprideis torosa, Tyrrhenocythere pontica, Tyrrhenocythere* sp., *T.* aff. *ruggierii, Loxoconcha petasa* and *L. muelleri*. Besides the dominance of *C. angulata* and *L. eichwaldi*, a few levels with an increasing presence of nodded *C. torosa* as well as *L. petasa* and *L. muelleri* are observed. Within the uppermost parts of the succession the valves are thicker and more ornate and *L. petasa* ssp. 1, *L. petasa* ssp.2, *Maeotcythere bosqueti, Amnicythere* sp. 1*, A.* sp. 2 and *C. torosa* are commonly occurring. Along the succession, rare occurrences of *Cypria* sp., *Candona* sp., as well as *Ilyocypris bradyi* and *I. gibba* suggest the minor influence of a neighbouring freshwater environment.

Denizli Phase 2, Unit 5: 17. *Caspiocypris carica*; 18. *Typhlocypris fossulata fossulata*; 19. *Typhlocypris fossulata reticulata*; 20.; *Typhlocyprella* sp.; 21. *Cypria* sp.; 22. *Tyrrhenocythere* aff. *pontica*; 23. *Cyprideis pannonica*; 24. *Amnicythere* ex. gr. *multituberculata*; 25. *Amnicythere striatocostata*; 26. *Amnicythere* aff. *striatocostata*; 27. *Leptocythere* sp.; 28. *Amnicythere* sp. 1; 29. *Amnicythere* sp. 3; 30. *Amnicythere* sp. 4; 31. *Loxoconcha babazananica*; 32. *Loxoconchissa (Loxocaspia)* aff. *reticulata*; (all specimens, except no.13, are left valves, external views, adults). Scalebar = 5 mm.

4.3.3. Palynology and dinoflagellates

The semi-quantitative results from palynomorph analyses and their environmental interpretations are reported in Table 1. In total, 16 samples were taken from all sedimentary units except for the coarse-grained unit 3. Four samples (all from Unit 4) did not contain any representative palynomorphs or dinocysts that would provide a palaeoenvironmental assessment and these are thus defined as barren.

The palynological assemblage of Unit 1 (seven samples) is dominated by dinoflagellates *Achomosphaera* and *Spiniferites* that indicate meso-to low euhaline salinity levels. Two samples from prodelta mudstones (DZZ_5 and DZB_5) display lower oligo-to mesohaline salinity.

The only sample analysed from Unit 2 (CS_11) is dominated by psilate inaperturate sphaerids (possibly *Leiosphaeridium*), that may belong to freshwater algae, although taxonomic definition is highly uncertain due to the absence of diagnostic features. Together with rare *Botryococcus* algae and abundant plant detritus, this assemblage indicates freshwater environments, likely representing a river pulse.

Unit 3 has not been sampled for palynology due to the coarse-grained lithology, and samples from Unit 4 are barren. Four samples from Unit 5 are generally dominated by the freshwater algae *Botryococcus* and *Pediastrum*, along with common mesohaline dinocysts, such as *Spiniferites, Achomosphaera,* and *Impagidinium* (Table 1). This may point towards mesohaline environments with significant freshwater input.
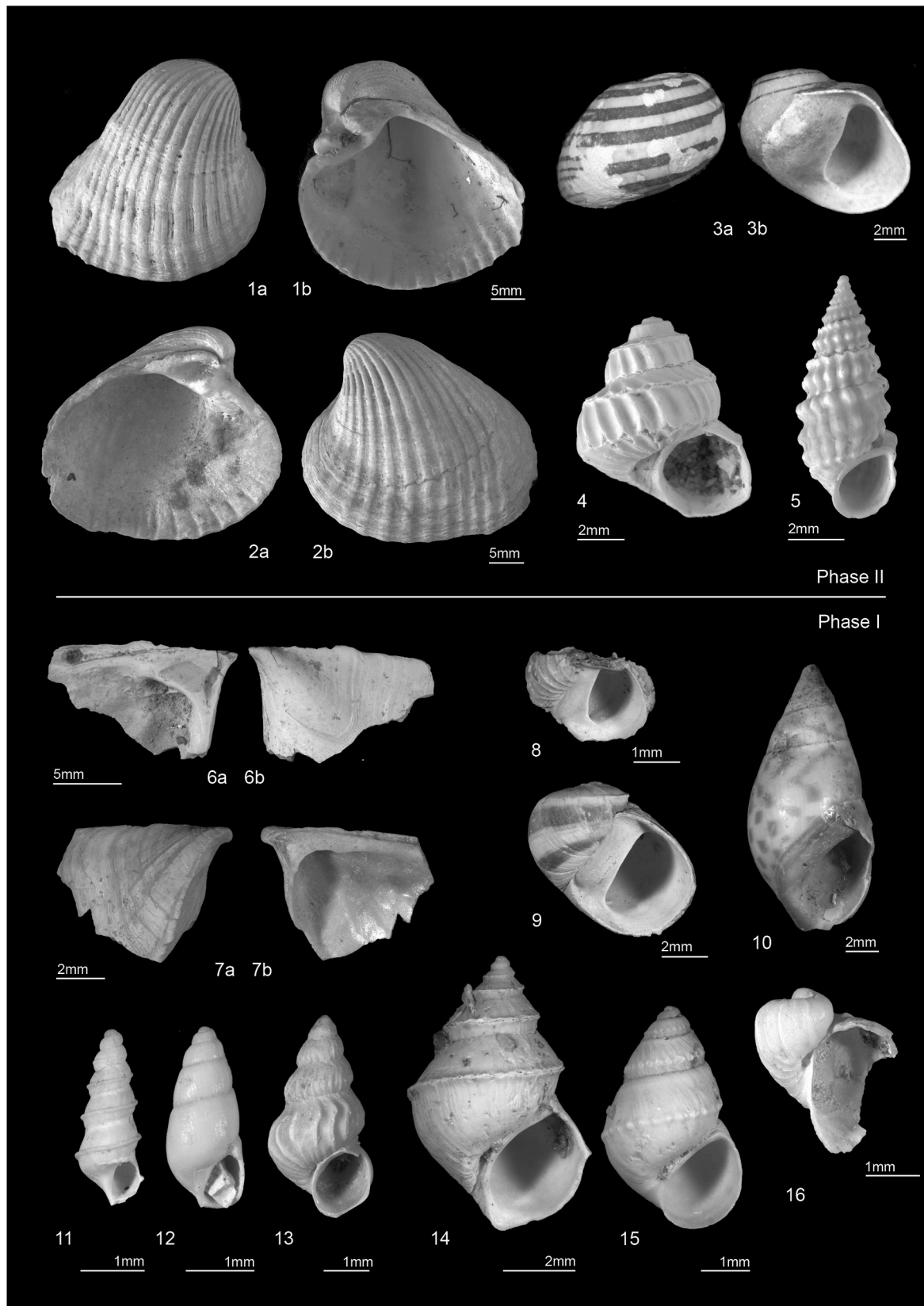
Fig. 5. Representative mollusc species from the studied outcrops in the Denizli Basin: (1) *Didacna phrygica*; (2) *Didacna elongata* (= an unreplaced junior homonym of *Didacna rudis* var. *elongata*); (3) *Theodoxus bukowskii*; (4) *Valvata cincta*; (5) "*Micromelania*" *phrygica*; (6) *Dreissena kairanderensis*; (7) *Dreissena* sp. 1 sensu Neubauer and Wesselingh (2023); (8) *Theodoxus* aff. *pilidei*; (9) *Theodoxus percarinatus*; (10) *Esperiana esperi*; (11) *Iraklimelania submediocarinata*; (12) *Prososthenia* cf. *sturanyi communis*; (13) *Harzhauseria schizopleura*; (14) *Falsipyrgula*? *coronata*; (15) *Falsipyrgula* cf. *sieversi*; (16) *Corymbina elegans* (1–5 from Wesselingh et al., 2008; 6–16 from Neubauer and Wesselingh, 2023).
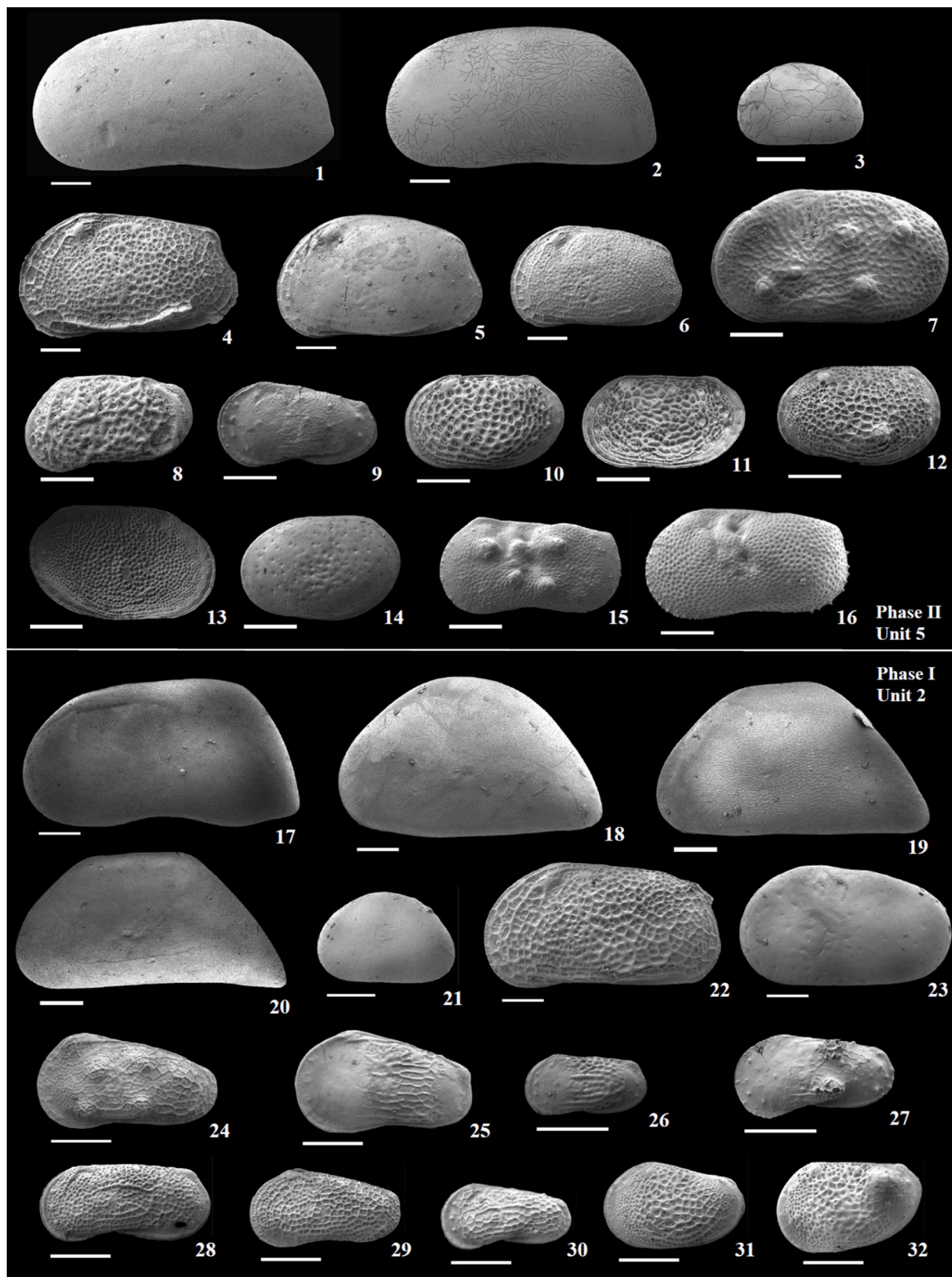
Fig. 6. Representative ostracod species from the studied outcrop. Denizli 1 Phase, Unit 2: 1. *Candona angulata*; 2. *Candona* ex. gr. *angulata*; 3. *Cypria* sp.; 4. *Tyrrhenocythere pontica*; 5. *Tyrrhenocythere* aff. *rugieri*; 6. *Tyrrhenocythere* sp. 7. *Cyprideis* ex. gr. *torosa*; 8. *Maetocythere bosqueti*; 9. *Amnicythere* sp. 2; 10. *Loxoconcha petasa*; 11. *Loxoconcha* ex. gr. *petasa*; 12. *Loxoconcha* ex. gr. *petasa* ssp. 1; 13. *Loxoconcha* ex. gr. *eichwaldi*; 14. *Loxoconcha muelleri*; 15. *Ilyocypris bradyi*; 16. *Ilyocypris gibba*.

Table 1
Summary of palynological analysis of samples from the Denizli outcrops.

Code	Strat. level, m	Dep. Unit	Description	Interpretation
BD_96	848.8	**5**	**Terrestrial**: *Pinus* (very abundant) **Aquatic**: *Botryococcus* (rare), *Achomosphaera* (rare)	Mesohaline offshore environments with minor freshwater influence
BD_58	829	**5**	**Terrestrial**: *Pinus* (common), *plant material* (rare) **Aquatic**: *Botryococcus* (abundant), *Spiniferites* spp. (present, more abundant than in the previous sample, some *S. cruciformis*, some *Spiniferites* with short processes)	Mesohaline neritic environments with freshwater influence
DZ_8	644	**5**	**Terrestrial**: *Pinus* (abundant), Amarathaceae (reworked), Poaceae (rare), *Abies* (rare) **Aquatic**: *Botryococcus* (abundant), *Spiniferites* (rare, some *S. cruciformis*), *Impagidinium spongianum* (rare), indet. transparent round palynomorphs	Mesohaline with significant freshwater influence
BDB_35	720.9	**5**	**Terrestrial**: *Pinus, Quercus*, Asteroideae, Poaceae, Amaranthaceae **Aquatic**: *Botryococcus* (very abundant), *Pediastrum* (very abundant), dinocysts (common) including *Caspidinium rugosum, Spiniferites (S. bentorii), Achomosphaera* spp., *Impagidinium spongianum,* cf. *Senegalinium,* cf. *Batiacasphaera*	Mesohaline with strong freshwater influence
CS_11	126.7	**2**	**Terrestrial**: *Pinus, Quercus*, Amaranthaceae, leaf fragments **Aquatic**: *Leiosphaeridium* (common), *Botryococcus* (rare)	Freshwater nearshore (?)
CS_2	100	**1**	**Terrestrial**: *Pinus* (present), *Quercus* (rare), Poaceae (rare) **Aquatic**: *Spiniferites* (abundant), *Achomosphaera* (abundant), *Polysphaeridium zoharyi* (common), *Lingulodinium machaerophorum* (common), *Botryococcus* (occasional)	Meso- to euryhaline, coastal/lagoonal
DZB_5	97.2	**1**	**Terrestrial**: abundant pollen and plant material, likely reworked **Aquatic**: *Botryococcus* (abundant), *Spiniferites cruciformis* (rare)	Oligo- to mesohaline, near-shore
DZZ_5	21	**1**	**Terrestrial**: *Pinus* (abundant), Poaceae (abundant), *Quercus* (rare), Lactucoideae (rare), Cupressaceae (rare), plant detritus, fungal spores **Aquatic**: cf. *Senegalinium* (rare), *Pterospermella* (rare)	Oligo- to mesohaline, near-shore
DBI_6	5	**1**	**Terrestrial**: *Pinus* (abundant), Asteraceae (occasional) **Aquatic**: *Spiniferites* (abundant), Achomosphaera (abundant), Thalassiphora? (rare).	Meso- to low euhaline, neritic with minor freshwater influence
DBI_3	2	**1**	**Terrestrial**: *Pinus* (abundant). **Aquatic**: *Spiniferites* (abundant), *Botryococcus* (rare), *Pediastrum* (rare)	Meso- to low euhaline, neritic with minor freshwater influence
DZZ_1	0.6	**1**	**Terrestrial**: *Pinus* (abundant), Poaceae (occasional), *Abies* (rare), **Aquatic**: *Achomosphaera* (abundant), *Impagidinium,* cf. *Pyxidinopsis*	Meso- to low euhaline, offshore
DBI_1	0	**1**	**Terrestrial**: *Pinus* (abundant) **Aquatic**: *Spiniferites* (abundant), *Botryococcus* (rare)	Meso- to low euhaline, neritic with minor freshwater influence

4.4. Interbasinal connectivity proxies

4.4.1. Bulk δ^{18}O and δ^{13}C

Within Unit 1, $\delta^{18}O$ (VPDB) values range between −6.63 and −2.9 ‰ (mean = −5.50 ‰) and $\delta^{13}C$ values range between −0.8 and 2.96 ‰ (mean = 1.55 ‰) for 16 samples (Fig. 7A). The covariation coefficient R is equal to 0.62 (Supplementary 1).

Compared to Unit 1, Unit 2 shows higher $\delta^{18}O$ and $\delta^{13}C$ values, ranging from −5.84 to −1.97 ‰ for $\delta^{18}O$ (mean = −4.09 ‰) and from 0.21 to 5.34 ‰ for $\delta^{13}C$ (mean = 2.82 ‰) for N = 24. Covariation between $\delta^{13}C$ and $\delta^{18}O$ is moderately positive and equal to 0.54. In Unit 3, only one sample from a thin marlstone layer could be measured due to its coarse-grained lithology. Both $\delta^{13}C$ and $\delta^{18}O$ values for this sample fall within the range of Unit 2.

In Unit 4, the $\delta^{18}O$ ratios fluctuate between −5.79 and −2.66 ‰ (mean = −4.09 ‰) and $\delta^{13}C$ ratios range from 0.41 to 3.02 ‰ (mean = 1.94 ‰) for N = 13 (Fig. 7). The R coefficient is at its maximum in the entire outcrop (0.91, Supplementary 1). The uppermost Unit 5 is generally characterised by very little variation in the isotope ratios. In Unit 5, the $\delta^{18}O$ ratios range from −4.97 to −3.17 ‰ (mean = −4.15 ‰) and $\delta^{13}C$ ratios - from 0.43 to 2.71 ‰ (mean 1.87 ‰) for N = 9.

4.4.2. $^{87}Sr/^{86}Sr$

Six strontium isotope ($^{87}Sr/^{86}Sr$) ratios measured on ostracods from lower Kolankaya (samples DZZ6, CS2, CS8, CS14) and upper Kolankaya deposits range from 0.7081 to 0.7082 (Table 2). These $^{87}Sr/^{86}Sr$ values from the Denizli Basin are significantly below marine values and also below Paratethys/Pontocaspian values from ostracods of the Black Sea Basin and Caspian Sea Basin (Fig. 7C).

5. Discussion

5.1. New age data driving reappraisal of the Denizli Basin evolution

The magnetic polarity pattern of the studied section comprises five normal polarity and six reversed polarity zones (Fig. 3). The $^{40}Ar/^{39}Ar$ age of 2.36–2.25 Ma of the volcanic tephra at 114 m allows correlation of the polarity zones in the following way: the lowermost N1-to-R1 polarity switch is correlated to the Gauss-Matuyama reversal dated at 2.61 Ma (Raffi et al., 2020); the N2 and N3 zones separated by the coarse-grained Unit 3 then likely represent one single normal polarity chron that we correlate to C2n (Olduvai, 1.934–1.775 Ma) (Fig. 8A). The Reunion subchron was not detected. Above, the series of numerous reversed polarity zones (R2–R5) separated by gaps is correlated to the upper part of the reversed Matuyama chron (C1r), enclosing the time interval between 1.77 and 0.78 Ma. The normal polarity subchrons Cobb Mountain and Jaramillo are missing, probably due to the large number of gaps in the upper half of the outcrop. The uppermost normal zone N4 is correlated to the Brunhes chron (C1n). The combination of palaeomagnetic and $^{40}Ar/^{39}Ar$ dating thus indicates an Early Pleistocene age of the studied succession of the Kolankaya Formation (Fig. 8A).

The new age strongly deviates from earlier Late Miocene estimates (Alçiçek et al., 2007; Wesselingh et al., 2008; Rausch et al., 2020), with major implications for the Aegean–Pontocaspian hydrological and palaeobiogeographic histories. The Late Miocene age estimates for the Kolonkaya Formation all strongly relied on the presence of the Turolian (MN11–12) Babadağ mammal locality located near Babadağ city (Yalçınlar, 1983). The similarity of the ostracods from Unit 2 with those of the Pannonian Basin type was also not in disagreement (Rausch et al., 2020). However, the exact stratigraphic relation between the studied outcrop and the Babadağ mammal locality is ambiguous as neither the exact geographic nor stratigraphic positions of the fossil site is known. The base of the studied outcrop is located ~2 km to the northwest from the Babadağ city and the outcrop in between is not well-exposed. Therefore, stratigraphic continuity between the Late Miocene mammal locality and the Early Pleistocene base of our section cannot be confirmed.

The new $^{40}Ar/^{39}Ar$ ages performed on four mineral fractions from different parts of the tephra layer (114 m, Fig. 8A) show an age range of 2.25–2.36 Ma. Even though it is hard to indicate precisely the eruption
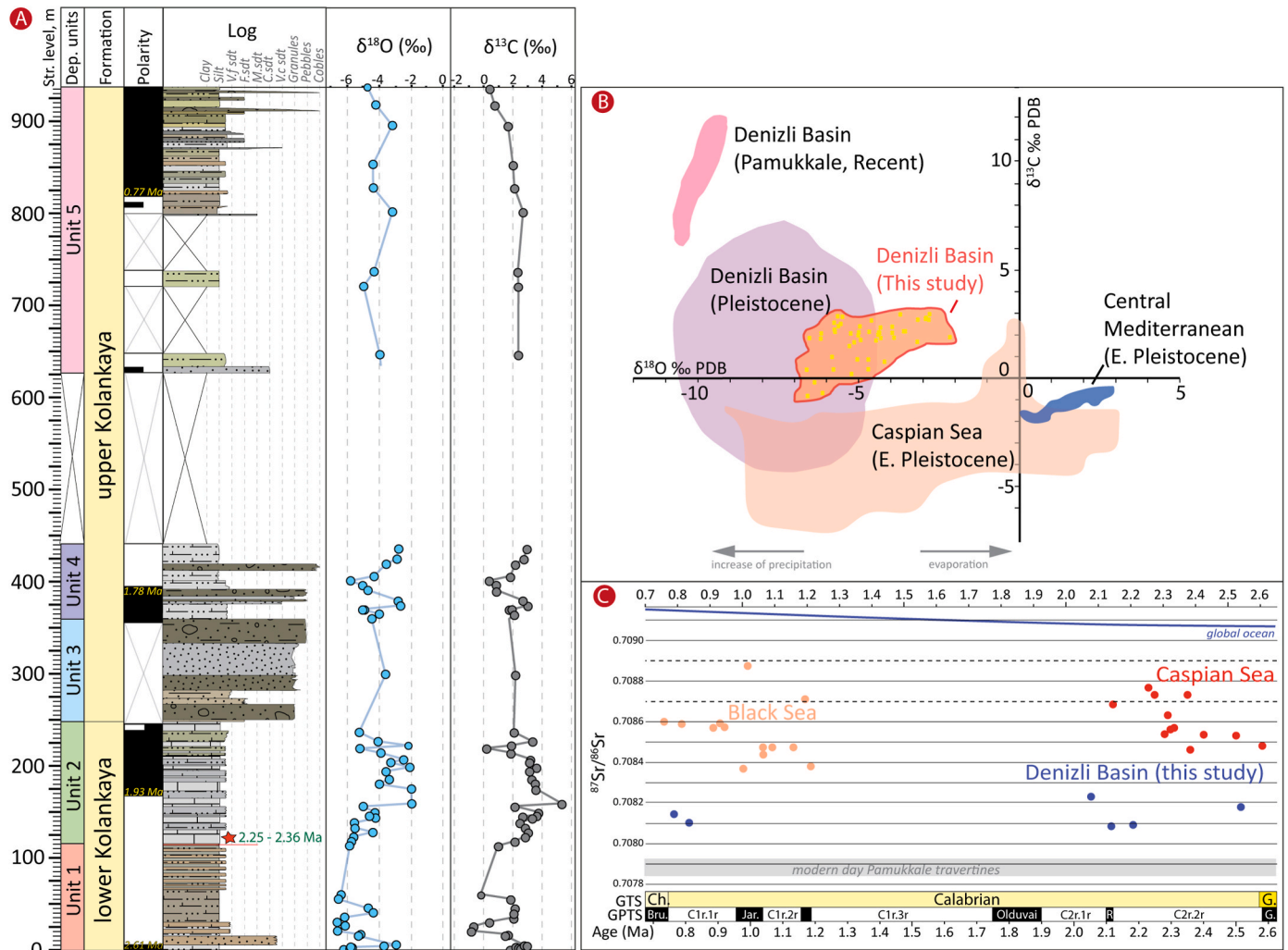
Fig. 7. Results on the δ^{18}O, δ^{13}C and [87]Sr/[86]Sr from the studied record and their comparison with other regional studies. A. Composite log and the δ^{18}O- and δ^{13}C-curves; B. Plot of the δ^{18}O, and δ^{13}C values and their comparison with other regional data: Denizli Basin (Pleistocene) and Pamukkale travertines (recent) (Boever et al., 2017); Caspian Sea (Early Pleistocene) (Jorissen, 2020); Central Mediterranean (Early Pleistocene) (Joannin et al., 2007). C. Plot of the [87]Sr/[86]Sr data from the studied outcrop (blue dots) and their comparison with the data from the Caspian Sea (Bista, 2019), the Black Sea (Bista et al., 2021), global ocean (thin blue line) (McArthur et al., 2020), and modern-day travertine from Pamukkale (grey bar) (Claes et al., 2015).

Table 2
[87]Sr/[86]Sr ratios in selected stratigraphic intervals of the studied section.

| Sample code	Stratigraphic level, m	Extrapolated age, Ma	[87]Sr/[86]Sr
BA23	826.9	0.76	0.708145
BD4	801.7	0.81	0.708104
CS14	129.8	2.05	0.708231
CS8	115.5	2.12	0.708087
CS2	100	2.18	0.708092
DZZ6	25	2.52	0.708182

age, similar age volcanic and volcaniclastic deposits were documented in other SW Anatolian basins, such as Kula volcanics in the Gediz Graben (2 Ma and younger, Bozkurt, 2003) and a volcanic tephra in the Söke-Milet Basin (2.4–2.25 Ma, Sümer et al., 2012), the latter being potentially identical to our tephra. Our palaeomagnetic data reveal a normal polarity interval above the tephra level, most likely corresponding to the Olduvai chron. In conclusion, combining two dating techniques helped solidify the age of the studied succession between 2.6 and 0.5 Ma and indicates an Early Pleistocene age for the studied portion of the Kolankaya Formation.

5.2. Early Pleistocene ecosystem evolution in the Denizli Basin

The Denizli Basin underwent a major palaeoenvironmental change in the Early Pleistocene. Two distinct lake phases, Denizli 1 (Units 1, 2) and Denizli 2 (Units 4,5), occurred with a major environmental transition during the Olduvai chron (Unit 3) that coincided with a faunal turnover event (Fig. 8B). The depositional settings of the lower (Denizli 1) and upper (Denizli 2) lake phases were very similar; the overall ecology of the benthic faunas indicate persistent oligohaline to mesohaline conditions. Yet, the ostracod and especially the mollusc faunas of Denizli Phase 1 were almost completely replaced in Denizli Phase 2.

Lake phase Denizli 1 is composed of prodeltaic siltstone and sandstone facies (Unit 1) and distal lacustrine marlstone-limestone facies (Unit 2) (FA7 and FA9, respectively in Alçiçek et al., 2007). The palynological composition of Unit 1 indicate oligohaline–mesohaline nearshore to offshore environments (Table 1). The δ^{18}O and δ^{13}C isotopes show relatively strong variations of 4‰ and a positive covariance pointing at a closed lake system (Meijers et al., 2020). A mean δ^{18}O ratio of −5.5‰ implies proximity of freshwater sources, while a short negative incursion of δ^{13}C from 3‰ to −0.8‰ suggest either a decrease of productivity or supply of lighter riverine [12]C (Li and Ku, 1997; Horton et al., 2016). Unit 2 is a distal lacustrine unit with interfingering distal
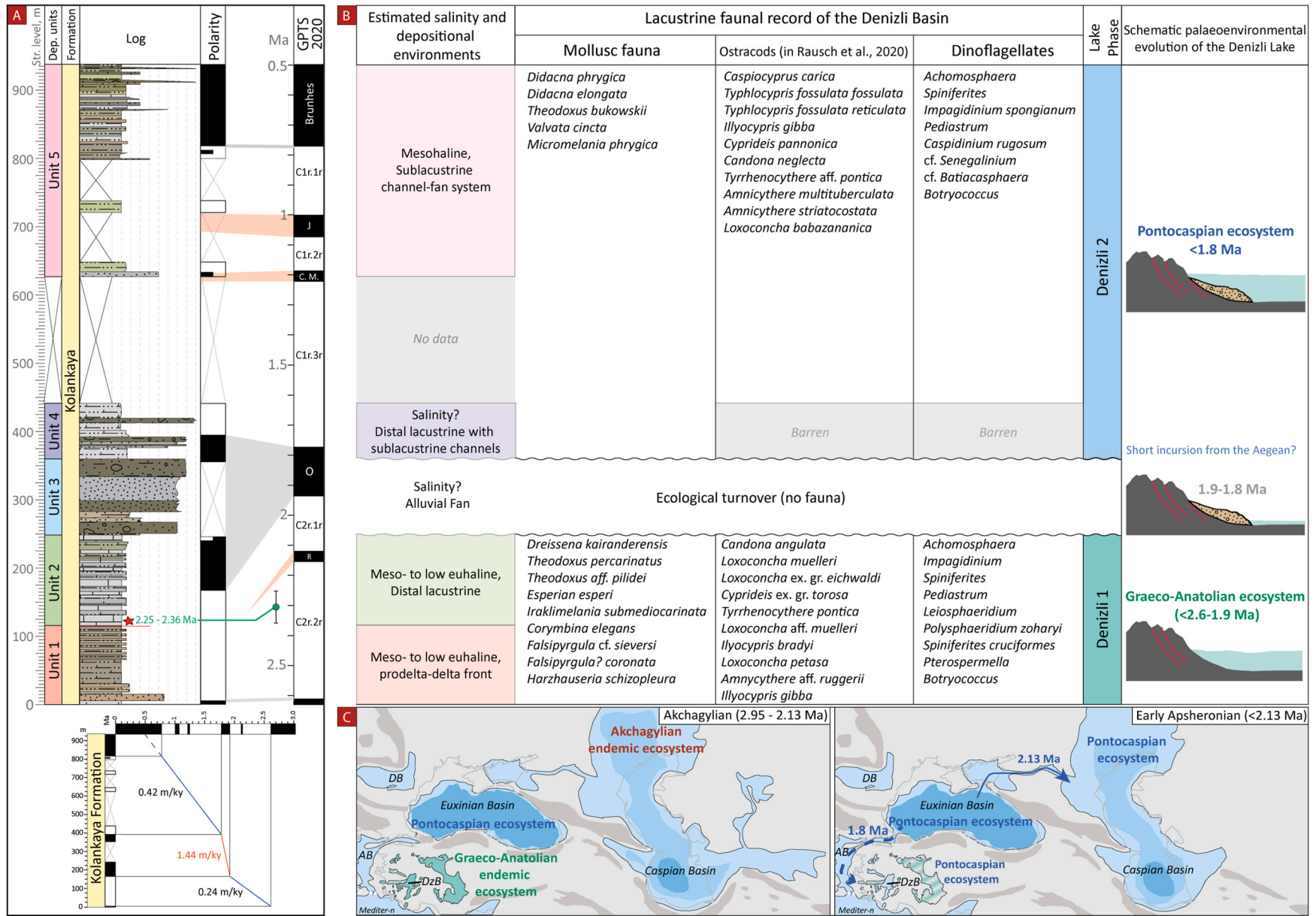
Fig. 8. Summary on the age, palaeoenvironments and faunal content of the studied outcrop. A. Correlation of the acquired polarity patterns and $^{40}Ar/^{39}Ar$ tephra age to the Global polarity Time Scale (GPTS) and estimation of the average sedimentation rates. B. Estimated salinity, depositional settings and faunal contents within the studied outcrop. C. Palaeogeographic map of the Anatolian and Pontocaspian areas in the Early Pleistocene with an indication of the Pontocaspian ecosystem expansion to the Caspian Sea at 2.13 Ma (Lazarev et al., 2019) and to the Denizli Basin at 1.8 Ma (this study). Palaeogeographic map is based on (Lüttig and Steffens, 1975; Popov, 2004).

delta lobes (Alçiçek et al., 2007). Mollusc and ostracod faunas also represent mesohaline–oligohaline conditions and are highly endemic, indicating the isolated nature and long duration (long-lived lake) of Lake Denizli during this phase. The δ^{13}C in Unit 2 is shifting towards positive ratios that fit distal lacustrine settings and may be indicative of an increase of evaporation and productivity, or alternatively, the remoteness from or decrease of freshwater input (Li and Ku, 1997; Horton et al., 2016)

Lake phase Denizli 2 is composed of distal lacustrine marlstones interbedded with conglomeratic incision fills of sublacustrine channels (Lazarev, 2020). The ostracod and mollusc faunas have a Pontocaspian character (Wesselingh et al., 2008; Rausch et al., 2020) and represent oligohaline to mesohaline salinities, which is confirmed by palynological data. The 3‰ oscillations of δ^{18}O generally follow the same trend as the changes in sedimentary facies with higher ratios in the distal lacustrine marlstones and lower ratios within the sublacustrine channels (Fig. 7). Unit 4 has the highest covariance coefficient of 0.91 suggesting that the lake had a maximum hydrological closedness and was controlled by the evaporation/precipitation balance (Li and Ku, 1997). The occurrence of Pontocaspian mollusc taxa in Unit 4 implies at least a short connection to another basin at the onset of the phase. Within the uppermost Unit 5, the palaeoenvironments are similar to Unit 4, except that the δ^{18}O and δ^{13}C values exhibit very low covariance (0.21, Supplementary 1), characterising a higher role of groundwater/inflow in the isotopic water composition (Li and Ku, 1997). Denizli Lake Phase 2 represents an isolated, long-lived Pontocaspian satellite lake.

The major turnover event must have occurred during the deposition of Unit 3. That unit is built of thick clast-supported massive to stratified conglomerates, suggesting accumulation in a highly dynamic alluvial fan/delta environment (Miall, 1996), characteristic for the tectonically active intermountain basins of Anatolia (Goktas and Hakyemez, 2000; Deynoux et al., 2005; Çiftçi and Bozkurt, 2009; Kieft et al., 2010). The sudden progradation of the alluvial fan could be linked with an extensional pulse in the basin reflected in the formation of a hanging wall along the propagating normal fault in the basin-bounding Babadağ fault zone (Gawthorpe and Leeder, 2000; Kaymakci, 2006). On the other hand, the progradation of alluvial fans may be a response to the climatically-driven decrease of the lake water level. The palynological analysis of the Plio-Pleistocene deposits from the neighbouring Çameli and Karacasu Basins generally indicates vegetation, characteristic for arid climate as well as humid-arid climate cyclicity correlated to glacial-interglacial cycles (Jiménez-Moreno et al., 2015). However, no extreme arid events were documented that could explain a major Denizli Lake level drop.

While the driver of Unit 3 alluvial fan progradation remains uncertain, it is clear that this unit delimits two distinct Lake phases with different faunal assemblages. The rebound in lake level, accompanied by the occurrence of the first *Didacna* molluscs, happened within the uppermost part of the Olduvai chron and is dated 1.8 Ma.

5.3. Palaeobiogeographic affinity of dinoflagellates and ostracods before and after turnover

The dinoflagellate assemblages of both the Denizli Phase 1 and Phase 2 are generally dominated by the genera *Spiniferites* and *Achomosphaera* (Table 1). These genera have a modern global distribution and commonly represent meso-to euhaline salinities (Zonneveld et al., 2013). However, both have their unique taxa delimited by the turnover event of Unit 3 (Table 1). Occurring uniquely in the Denizli Phase 1, *Polysphaeridium zoharyi* and *Lingulodinium machaerophorum* are nowadays found in near-coast brackish areas around the world (Zonneveld et al., 2013). Both taxa were documented in the Paratethyan/Pontocaspian region in Upper Miocene–Early Pleistocene deposits (Soliman and Riding, 2017; Hoyle et al., 2018, 2021). The Denizli Phase 2 assemblage comprises *Impagidinium spongianum* and *Caspidinium rugosum* (Table 1), which are characteristic Paratethyan/Pontocaspian

taxa, typically representing oligo-mesohaline coastal areas (Hoyle et al., 2021).

The overview of the dinocysts assemblage from the Denizli record suggests that Denizli Phase 1 contains global and Paratethyan taxa that had lived in the Central European Lake Pannon and the Eastern Paratethys since the Late Miocene and could subsequently have migrated to the Denizli Lake. The occurrence of Pontocaspian endemic dinoflagellates during Denizli Phase 2 implies a short incursion from the Pontocaspian area.

The ostracod assemblage from Denizli Phase I (Unit 2) also contains species of Late Miocene affinities of the Pannonian Basin (Jiřiček, 1985), the Dacian Basin (Olteanu, 1989; Stoica et al., 2013; van Baak et al., 2015; Lazarev et al., 2020; Matoshko et al., 2023) and the Euxinian Basin (Tunoglu and Ünal, 2001; Matzke-Karasz and Witt, 2005). The common genus *Typhlocypris* (*T. fossulata fossulata, T. fossulata reticulate*) and *Typhlocyprella* sp. are Paratethyan brackish water ostracods known from the upper Pannonian of the Vienna Basin (Sokač, 1972; Krstić, 1973), Pontian of Türkiye (Tunoğlu, 2003) and many other Paratethyan localities (Carbonnel, 1969; Vekua, 1975; Freels, 1980; Pipík and Bodergat, 2007).

A big change in the faunal composition takes place between Lake Phase I and Lake Phase II. While all the taxa still have a Paratethyan/Pannonian origin, several new ostracods such as *Amnicythere multituberculata*, *A. striatocostata* and *Loxoconcha babazananica* are common species in the Early Pleistocene record of the South Caspian Basin, in particular in Akchagylian–Apsheronian deposits dated between 2.95 and 0.85 Ma (van Baak et al., 2013, 2019; Lazarev et al., 2019).

In summary, all faunal groups in the Denizli Phase 1 demonstrate Paratethyan/Pannonian and Aegean-Anatolian affinities, while in Phase 2, together with Paratethyan groups, new Pontocaspian faunal elements common for the Early Pleistocene Caspian Sea occur in the record.

5.4. Geochemical traces of water incursion into the Denizli Basin

The invasion of new faunal assemblages in the Denizli Basin at 1.8 Ma raises a question about the connectivity of the Denizli Basin at the time. The ^{87}Sr/^{86}Sr ratio is a tool allowing to trace the water input source (e.g. riverine, incursion from neighbouring basins or global ocean) (McArthur et al., 2020). The ^{87}Sr/^{86}Sr value of the Denizli basin range from 0.7081 to 0.7082, much lower compared to the Early Pleistocene ^{87}Sr/^{86}Sr values from the Black Sea (Bista et al., 2021) and the Caspian Sea (Bista, 2019). In addition, these values are significantly below the global ocean values (McArthur et al., 2020), indicating no major incursion from these sources within the studied intervals (Fig. 7C). No overlap was found with the ^{87}Sr/^{86}Sr values from the modern day Pamukkale travertines of the Denizli Basin (Claes et al., 2015), indicating a different Sr-source in the Early Pleistocene Denizli Lake, enriched in heavier ^{87}Sr.

The reconstruction of covariance between δ^{18}O and δ^{13}C is a powerful tool that can provide information about the hydrological closedness or openness of the lake. In hydrologically closed basins, the water balance (precipitation vs. evaporation) remains stable over time, and thereby, the δ^{18}O and δ^{13}C demonstrate similar trends (positive covariance), while changes in the water balance (e.g. increase of riverine or groundwater exchange, outflow or connection to the neighbouring basins) tend to disrupt the δ^{18}O and δ^{13}C (negative covariance) indicating the hydrological openness of the basin (Li and Ku, 1997; Meijers et al., 2020). In all stratigraphic units, the δ^{18}O and δ^{13}C display positive covariance, meaning that the basin was hydrologically closed, although moderate and weak R values were acquired in Units 1,2 and especially 5 (R = 0.21), suggesting that the Denizli Lake might have a limited hydrological exchange with the other basins (4.1, Supplementary 1). Remarkably, the highest R of 0.91 was measured in the post-turnover Unit 4. This suggests the basin reached the maximum hydrological closeness and that the hydrological disruption accompanied by the biotic turnover episode indeed happened within Unit 3. It should also be

noted that a very short incursion that brought new Pontocaspian fauna at 1.8 Ma into the Denizli Lake could be a very short, pulse-like event. As suggested by Li and Ku (1997), very short and limited incursions may not affect the δ^{18}O and δ^{13}C isotopic content and may remain, therefore, undetected in the geochemical signature.

5.5. Pontocaspian fauna dispersal into SW Anatolia: the role of the Denizli Basin and potential dispersal pathways

The invasion of the Pontocaspian faunas into the Denizli Basin most likely happened within Unit 3, dated between 1.9 and 1.8 Ma, with the first documented *Didacna* shells dated to 1.8 Ma. The new ages allow us to better understand the palaeobiogeographic evolution of the Aegean–Anatolian–Pontocaspian region in the context of the key hydrological and biotic events of that time.

The first major expansion of the Pontocaspian ecosystems happened at 2.13 Ma, when the hydrological reconnection of the Black and Caspian Sea basins triggered an immigration wave of Pontocaspian faunal elements in the Caspian Sea Basin (Lazarev et al., 2019) (Fig. 8C). The impoverished endemic Akchagylian faunas of the Caspian Sea were replaced with more or less modern Pontocaspian assemblages. This strong ecological turnover marks the Akchagylian–Apsheronian boundary in the Caspian Sea (Krijgsman et al., 2019). The new age constraints from Denizli suggest that the Pontocaspian realm expansion also reached southwest Anatolia at 1.9–1.8 Ma (Fig. 8C).

The dispersal pathways of Paratethyan and Pontocaspian biota into SW Anatolia have long been uncertain. Besides Denizli, Pontocaspian faunal elements with characteristic mollusc species such as *Monodacna imrei* are known from the adjacent Baklan Basin (Wesselingh and Alçiçek, 2010) (Fig. 9). A recent study on the palaeoenvironments of Baklan stated that the Pontocaspian elements could have arrived from the Caspian Sea via the Black Sea and the Aegean Sea at 2.6 Ma during the so-called Akchagylian transgression (Alçiçek et al., 2023). However, the Akchagylian transgression started at 2.95 Ma (Lazarev et al., 2021) and peaked at 2.7 Ma (Krijgsman et al., 2019; van Baak et al., 2019). Moreover, during the Akchagylian, the Caspian Sea was inhabited by the endemic Akchagylian fauna that has little in common with the Pontocaspian assemblages (Krijgsman et al., 2019). Other Late Pleistocene faunas with lymnocardiids have been reported from the Konya Basin (Büyükmeriç and Wesselingh, 2018) but were explained as the result of avian dispersal. The latter mechanism, nevertheless, cannot explain a sharp and massive occurrence of different faunal Pontocaspian groups (molluscs, ostracods, dinocysts) in the Denizli Phase 2.

The geographic limitation of the Pontocaspian fauna in SW Anatolia (Denizli and Baklan Basins) allows us to speculate on the biogeographic dispersal paths. We propose three options: 1. A Black Sea - Denizli pathway via the Aegean Sea - Söke-Milet Basin (SMB) - Büyük Menderes Graben (BMG); 2. A Black Sea - Denizli pathway via the Aegean Sea – Izmir Bay (IB)- Gediz Graben (GG); 3. A direct intra-Anatolian pathway from the Black Sea (Fig. 9).

Option 1 (Söke-Milet Basin - Büyük Menderes Graben). *Didacna* has been reported from the Early Pleistocene succession of the Söke-Milet Basin deriving from shallow marine fan-deltaic deposits of the Fevzipaşa Formation (Sümer et al., 2012). However, illustrated specimens show in fact *Cerastoderma glaucum*, a species that occurs well beyond the Pontocaspian region and is not a reliable biogeographic marker. The shallow marine environments in the Söke-Milet Basin lasted from ~2.3 to 1.2 Ma, correlating to Units 2–5 in our outcrop, including the 1.8 Ma biotic turnover event.

The Early Pleistocene record of the Büyük Menderes Graben (BMG) is unresolved due to the lack of a common stratigraphic scheme and the absence of reliable geochronological constraints. The biochronological study of Sarica (2000) indicates the presence of marlstones and fine-grained mudstones in the depositional record. Another study shows that the Early Pleistocene record of the BMG is represented by the Arzular Formation with a Hıdırbeyli Member being lacustrine in origin
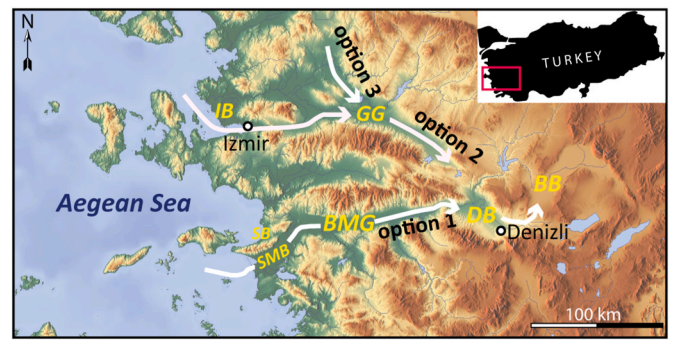

Fig. 9. Potential Pontocaspian fauna migration pathways into the Denizli and Baklan basins. Abbreviations: DB – Denizli Basin, BB – Baklan Basin, BMG – Büyük Menderes Graben; GG – Gediz Graben, IB – Izmir Bay; SB – Söke basin, SMB – Söke-Milet Basin. The map base is taken from www.maps-for-free.com.

(Goktas and Hakyemez, 2000). These lacustrine deposits would be a good candidate for hosting the Aegean-Denizli connection; however, no Pontocaspian faunas have been reported from them to this date.

Option 2 (Izmir Bay – Gediz Graben) is a less favourable route as the Early Pleistocene record of both, the Izmir Bay and the Gediz Graben are built of alluvial fan conglomerates (Bozkurt and Sözbilir, 2004; Uzel et al., 2012). At the same time, the tectonic reconstructions from the Izmir Bay show that in the Early Pleistocene, the area was flooded by the Aegean Sea (Uzel et al., 2012). In the Gediz Graben, the alluvial fans have a transverse origin, leaving the depositional environments of the axial part of the graben unclear (Bozkurt and Sözbilir, 2004).

Option 3 (Direct Black Sea—Denizli route) is an alternative scenario that is difficult to envisage based on literature data but suffers from incomplete knowledge of the sedimentary fill of the intervening basins. A basin route north from the Gediz Graben would end up in a block with Pre-Neogene basement rocks.

All three connectivity options remain highly speculative as all basins lack comprehensive palaeoenvironmental age constraints and incomplete understanding of the stratigraphic successions. We conclude that shallow marine and lacustrine deposits in the Söke-Milet Basin and Büyük Menderes basins, respectively, make this path tenable. Option 2 (Izmir Bay – Gediz Graben) cannot be fully excluded as even in the prevalence of alluvial fans, short water incursion from the Aegean Basin into the Denizli Basin could have taken place, with further erosion of its traces by active alluvial deposition.

Further, biogeographically important records exist in Greece that show a similar type of composition as the Denizli faunas. Shared among both are *Theodoxus*, melanopsids, the general high diversity of hydrobiids, *Valvata*, *Dreissena*, as well as *Didacna* species and *Corymbina elegans* (marker taxa for Denizli Phase 2 and Phase 1, respectively (Koskeridou and Ioakin, 2009). The Greek material has an Early to Middle Pleistocene age (Esu and Girotti, 2015, 2020) and emphasises the role of the Aegean region as a centre of the Pontocaspian biota during that time. The Greek faunas show, moreover, that no direct connection between the Denizli region and the Black Sea Basin was required to explain the introduction of the Pontocaspian biota in the former and thus exclude Option 3.

5.6. Implications of revised age constraints of the Kolankaya Formation in the Denizli Basin

The new age constraints of the Kolankaya Formation raise a question on the lithostratigraphic and geochronological subdivision of the Denizli Basin. Our new results demonstrate that the largest portion of the Kolankaya Formation, widely exposed in the southern part of the basin (Fig. 1), can no longer be considered a Miocene Unit but has a Pliocene–Early Pleistocene age. This principally breaks the existing stratigraphic scheme of the basin and points to the necessity of revision.

In addition, the relationships between the studied area and the nearby Late Miocene Babadağ mammal locality, the origin of the unconformity created by Unit 3 (alluvial fan), and the development of the transverse sublacustrine channel-fan system (Unit 4) must be reinvestigated from a tectonic point of view. All these sedimentary and structural features may be indicative of a previously unknown Pleistocene pulse of the Menderes uplift running along the Babadağ fault zone.

The biochronologically-derived age constraints of the Denizli Basin require an interdisciplinary revision, with the application of complementary dating methods (magnetostratigraphy and $^{40}Ar/^{39}Ar$ dating), sedimentary and biotic reconstructions. Our study sets a great example of how the power of an integrated stratigraphic approach can drastically change and improve previously accepted stratigraphic paradigms and bring new prospectives on the palaeobiogeographic and tectonic evolution of the sedimentary basins.

6. Conclusion

Integration of various dating ($^{40}Ar/^{39}Ar$, magnetostratigraphy), palaeoenvironmental (logging, palynology, mollusc and ostracod fauna) and geochemical ($^{87}Sr/^{86}Sr$, $\delta^{18}O$ and $\delta^{13}C$) proxies in a 937-m-thick record of the Kolankaya Formation of the Denizli Basin brings new insights into the Early Pleistocene dispersal of the Pontocaspian fauna in SW Anatolia and potential Aegean-Pontocaspian hydrological exchange. The Pleistocene part of the Kolankaya Formation comprises two lake phases (Denizli-1 and Denizli-2) with a major turnover event in between. During the lake phase Denizli 1, dated from 2.6 to 1.9 Ma, the Denizli Basin was occupied by an oligohaline-mesohaline lake with prodeltaic (Unit 1) and distal lacustrine settings (Unit 2). The biotic record indicates oligo-to mesohaline salinity, while the moderate positive covariance of $\delta^{18}O$ and $\delta^{13}C$ indicates a closed (underfilled) lake. During that time, the lake was inhabited by a mollusc fauna of Aegean-Anatolian affinity and dinoflagellates and ostracods of Pannonian/Paratethyan affinity. At 1.9 Ma, a sudden massive progradation of alluvial fans (Unit 3) characterises either a propagation pulse of the Babadağ Fault Zone or a climatically-driven lake-level drop. The palaeoenvironmental disruption terminated at 1.8 Ma and was marked by recovery of distal lacustrine settings with occasional sublacustrine channel fans (Units 3 and 4) and occurrence of principally new mollusc and ostracod fauna of Pontocaspian affinity. Palynological, ostracod and mollusc records imply mesohaline palaeosalinities, but with significant freshwater pulses. A strong positive covariation $\delta^{18}O$ and $\delta^{13}C$ suggests a hydrologically closed nature of the Deniizli Lake, that however, weakens towards the top of the section (Unit 5).

Comparison with major hydrological and biotic events in the Pontocaspian and Aegean regions suggests that the Denizli Basin played a limited role in the biogeographic evolution of the Pontocaspian biota. Dispersal of the Pontocaspian fauna into the Denizli Basin at 1.8 Ma likely occurred from the Black Sea Basin through the Aegean Sea Basin and a series of SW Anatolian graben basins (via Söke-Milet Basin - Büyük Menderes Graben or via the Izmir Bay-Gediz Graben). The confirmation of the hypothesised connectivity routes, however, requires a detailed multiproxy study in the abovementioned basins as they still miss comprehensive stratigraphic, geochronological and palaeoenvironmental constraints.

The new Early Pleistocene age constraint firmly refutes the previously proposed Miocene age of the studied portion of the Kolankaya Formation. The basin stratigraphy requires thorough revision and redating using a combination of different dating proxies. Our study creates a good example of how reliance on unclear biochronological constraints and endemic fauna can create a lasting erroneous scientific legacy concerning age constraints.

The dating of the Pontocaspian fauna in the Denizli Basin draws attention to the role of the Aegean Basin in shaping and establishing the modern Pontocaspian biota, hopefully encouraging new palaeoenvironmental studies in the Aegean region.

CRediT authorship contribution statement

Sergei Lazarev: Conceptualization, Data curation, Investigation, Methodology, Project administration, Validation, Visualization, Writing – original draft, Writing – review & editing. **Mehmet Cihat Alçiçek:** Data curation, Project administration, Resources, Writing – review & editing. **Lea Rausch:** Formal analysis, Investigation, Methodology, Visualization, Writing – original draft, Writing – review & editing. **Marius Stoica:** Formal analysis, Investigation, Methodology, Visualization, Writing – original draft, Writing – review & editing. **Klaudia Kuiper:** Formal analysis, Investigation, Methodology, Resources, Visualization, Writing – original draft, Writing – review & editing. **Thomas A. Neubauer:** Formal analysis, Investigation, Methodology, Visualization, Writing – original draft, Writing – review & editing. **Hemmo A. Abels:** Data curation, Methodology, Writing – review & editing. **Thomas M. Hoyle:** Formal analysis, Investigation, Methodology, Writing – original draft, Writing – review & editing. **Christiaan G.C. van Baak:** Data curation, Methodology, Project administration, Writing – review & editing. **Anneleen Foubert:** Formal analysis, Methodology, Writing – review & editing. **Diksha Bista:** Formal analysis, Investigation, Methodology, Writing – original draft, Writing – review & editing. **Francesca Sangiorgi:** Formal analysis, Methodology, Writing – review & editing. **Frank P. Wesselingh:** Conceptualization, Formal analysis, Funding acquisition, Investigation, Methodology, Project administration, Supervision, Visualization, Writing – original draft, Writing – review & editing. **Wout Krijgsman:** Conceptualization, Methodology, Resources, Supervision, Writing – review & editing.

Declaration of competing interest

The authors declare that they have no known competing financial interests or personal relationships that could have appeared to influence the work reported in this paper.

Acknowledgements

Appendix A. Supplementary data

Supplementary data to this article can be found online at https://doi.org/10.1016/j.quascirev.2024.109050.

Data availability

All data associated with this manuscript are attached as supplementary materials and are fully available for fourther re-use/share

References

Alçiçek, H., 2010. Stratigraphic correlation of the Neogene basins in southwestern Anatolia: regional palaeogeographical, palaeoclimatic and tectonic implications. Palaeogeogr. Palaeoclimatol. Palaeoecol. 291 (3–4), 297–318. https://doi.org/10.1016/j.palaeo.2010.03.002.

Alçiçek, H., Gross, M., Bouchal, J.M., Wesselingh, F.P., Neubauer, T.A., Meijer, T., van den Hoek Ostende, L.W., Tesakov, A., Murray, A.M., Mayda, S., Alçiçek, M.C., 2023. Paleobiodiversity and paleoenvironments of the eastern Paratethys pleistocene lacustrine-palustrine sequence in the Baklan Basinbasin (SW Anatolia, Turkey). Palaeogeogr. Palaeoclimatol. Palaeoecol. 626, 111649. https://doi.org/10.1016/j.palaeo.2023.111649.

Alçiçek, H., Jiménez-Moreno, G., 2013. Late Miocene to plio-pleistocene fluvio-lacustrine system in the Karacasu basin (SW Anatolia, Turkey): depositional, paleogeographic and paleoclimatic implications. Sediment. Geol. 291, 62–83. https://doi.org/10.1016/j.sedgeo.2013.03.014.

Alçiçek, H., Varol, B., Özkul, M., 2007. Sedimentary facies, depositional environments and palaeogeographic evolution of the Neogene Denizli Basin, SW Anatolia, Turkey. Sediment. Geol. 202 (4), 596–637. https://doi.org/10.1016/j.sedgeo.2007.06.002.

Alçiçek, H., Wesselingh, F.P., Alçiçek, M.C., 2015. Paleoenvironmental evolution of the late Pliocene–early Pleistocene fluvio-deltaic sequence of the Denizli Basin (SW Turkey). Palaeogeogr. Palaeoclimatol. Palaeoecol. 437, 98–116. https://doi.org/10.1016/j.palaeo.2015.06.019.

Alçiçek, M.C., Mayda, S., Veen, J.H. ten, Boulton, S.J., Neubauer, T.A., Alçiçek, H., Tesakov, A.S., Saraç, G., Hakyemez, H.Y., Göktaş, F., Murray, A.M., Titov, V.V., Jiménez-Moreno, G., Büyükmeriç, Y., Wesselingh, F.P., Bouchal, J.M., Demirel, F.A., Kaya, T.T., Halaçlar, K., Bilgin, M., van den Hoek Ostende, L.W., 2019. Reconciling the stratigraphy and depositional history of the Lycian orogen-top basins, SW Anatolia. Palaeobio Palaeoenv 99 (4), 551–570. https://doi.org/10.1007/s12549-019-00394-3.

Bista, D., 2019. Reconstructing the Pleistocene Connectivity History of the Black Sea and the Caspian Sea Using Strontium Iotopes. Doctoral Thesis. University of Bristol, Bristol.

Bista, D., Hoyle, T.M., Simon, D., Sangiorgi, F., Richards, D.A., Flecker, R., 2021. Sr isotope-salinity modelling constraints on Quaternary Black Sea connectivity. Quat. Sci. Rev. 273, 107254. https://doi.org/10.1016/j.quascirev.2021.107254.

Boever, E. de, Brasier, A.T., Foubert, A., Kele, S., 2017. What do we really know about early diagenesis of non-marine carbonates? Sediment. Geol. 361, 25–51. https://doi.org/10.1016/j.sedgeo.2017.09.011.

Bozkurt, E., 2003. Origin of NE-trending basins in western Turkey. Geodin. Acta 16 (2–6), 61–81. https://doi.org/10.1016/S0985-3111(03)00002-0.

Bozkurt, E., Sözbilir, H., 2004. Tectonic evolution of the Gediz Graben: field evidence for an episodic, two-stage extension in western Turkey. Geol. Mag. 141 (1), 63–79. https://doi.org/10.1017/S0016756803008379.

Büyükmeriç, Y., Wesselingh, F.P., 2018. New cockles (Bivalvia: cardiidae: lymnocardiinae) from late pleistocene lake karapınar (Turkey): discovery of a pontocaspian refuge? Quat. Int. 465, 37–45. https://doi.org/10.1016/j.quaint.2016.03.018.

Carbonnel, G., 1969. Les ostracodes du Miocène Rhodanien: Systématique, biostratigraphie écologique, paléobiologie. In: Documents des Laboratoires de Géologie de la Faculté des Sciences de Lyon 32. Lyon University, Lyon.

Çiftçi, N.B., Bozkurt, E., 2009. Structural evolution of the Gediz Graben, SW Turkey: temporal and spatial variation of the graben basin. Basin Res. 173, 385. https://doi.org/10.1111/j.1365-2117.2009.00438.x.

Claes, H., Soete, J., van Noten, K., El Desouky, H., Marques Erthal, M., Vanhaecke, F., Özkul, M., Swennen, R., 2015. Sedimentology, three-dimensional geobody reconstruction and carbon dioxide origin of Pleistocene travertine deposits in the Ballık area (south-west Turkey). Sedimentology 62 (5), 1408–1445. https://doi.org/10.1111/sed.12188.

Deynoux, M., Çiner, A., Monod, O., Karabıyıkoglu, M., Manatschal, G., Tuzcu, S., 2005. Facies architecture and depositional evolution of alluvial fan to fan-delta complexes in the tectonically active Miocene Köprüçay Basin, Isparta Angle, Turkey. Sediment. Geol. 173 (1–4), 315–343. https://doi.org/10.1016/j.sedgeo.2003.12.013.

Doğan, A., Mayda, S., Alçiçek, M., 2020. Denizli Havzası (GB Anadolu) Neojen istifinde ilk Turoliyen bulgusu ve bölgesel paleobiyocoğrafik önemi. Bulletin Of The Mineral Research and Exploration 162 (162), 1–10. https://doi.org/10.19111/bulletinofmre.651620.

Erten, H., Sen, S., Görmüş, M., 2014. Middle and Late Miocene Cricetidae (Rodentia, Mammalia) from Denizli Basin (Southwestern Turkey) and a New Species of Megacricetodon. J. Paleontol. 88 (3), 504–518. https://doi.org/10.1666/13-060.

Esu, D., Girotti, O., 2015. The late Early Pleistocene non-marine molluscan fauna from the Synania Formation (Achaia, Greece), with description of nine new species (Mollusca: gastropoda). archmoll 144 (1), 65–81. https://doi.org/10.1127/arch.moll/1869-0963/144/065-081.

Esu, D., Girotti, O., 2020. Updating a late Early – Middle Pleistocene non-marine molluscan fauna from Achaia (Greece). Systematics and palaeoecological remarks. Bollettino Malacologico 56, 59–83.

Fisher, R., 1953. Dispersion on a sphere. Proc. R. Soc. A 217 (1130), 295–305. https://doi.org/10.1098/rspa.1953.0064.

Freels, F., 1980. Limnische Ostrakoden aus Jungtertiar und Quartar der Turkei. Geol. Jahrb. 39, 3–169.

Gautier, P., Brun, J.-P., Moriceau, R., Sokoutis, D., Martinod, J., Jolivet, L., 1999. Timing, kinematics and cause of Aegean extension: a scenario based on a comparison with simple analogue experiments. Tectonophysics 315 (1–4), 31–72. https://doi.org/10.1016/S0040-1951(99)00281-4.

Gawthorpe, R.L., Leeder, M.R., 2000. Tectono-sedimentary evolution of active extensional basins. Basin Res. 12 (3–4), 195–218. https://doi.org/10.1111/j.1365-2117.2000.00121.x.

Goktas, F., Hakyemez, H.Y., 2000. Late Pliocene-Pleistocene Stratigraphy of the Büyük Menderes Graben Fill, Western Turkey.

Gramann, F., Kockel, F., 1969. Das Neogen im Strimonbecken (Griechisch-Ostmazedonien), Teil 1: Lithologie, Stratigraphie und Paläogeographie. Verlag nicht ermittelbar.

Horton, T.W., Defliese, W.F., Tripati, A.K., Oze, C., 2016. Evaporation induced 18O and 13C enrichment in lake systems: a global perspective on hydrologic balance effects. Quat. Sci. Rev. 131, 365–379. https://doi.org/10.1016/j.quascirev.2015.06.030.

Hoyle, T.M., Leroy, S.A., López-Merino, L., Richards, K., 2018. Using fluorescence microscopy to discern in situ from reworked palynomorphs in dynamic depositional environments — an example from sediments of the late Miocene to early Pleistocene Caspian Sea. Rev. Palaeobot. Palynol. 256, 32–49. https://doi.org/10.1016/j.revpalbo.2018.05.005.

Hoyle, T.M., Leroy, S.A., López-Merino, L., van Baak, C.G., Martínez Cortizas, A., Richards, K., Aghayeva, V., 2021. Biological turnovers in response to marine incursion into the Caspian Sea at the Plio-Pleistocene transition. Global Planet. Change 206, 103623. https://doi.org/10.1016/j.gloplacha.2021.103623.

Jiménez-Moreno, G., Alçiçek, H., Alçiçek, M.C., van den Hoek Ostende, L., Wesselingh, F. P., 2015. Vegetation and climate changes during the late Pliocene and early Pleistocene in SW Anatolia, Turkey. Quat. res. 84 (3), 448–456. https://doi.org/10.1016/j.yqres.2015.09.005.

Jiriček, R., 1985. Die Ostracoden des Pannonien. In: Papp, A., Jámbor, Á., Steininger, F. F. (Eds.), Miozän der Zentralen Paratethys. Pannonien: Slavonien und Serbien. Akadémiai Kiadó, Ungarische Akademie der Wissenschaften, Budapest, pp. 378–425.

Joannin, S., Quillévéré, F., Suc, J.-P., Lécuyer, C., Martineau, F., 2007. Early Pleistocene climate changes in the central Mediterranean region as inferred from integrated pollen and planktonic foraminiferal stable isotope analyses. Quat. res. 67 (2), 264–274. https://doi.org/10.1016/j.yqres.2006.11.001.

Jorissen, E.L., 2020. The Pontocaspian basins in a grain of sand: coastal sedimentary architecture, forcing mechanisms, and faunal turnover events in restricted basins. PhD. Utrecht University, Utrecht (PhD).

Kaymakci, N., 2006. Kinematic development and paleostress analysis of the Denizli Basin (Western Turkey): implications of spatial variation of relative paleostress magnitudes and orientations. J. Asian Earth Sci. 27 (2), 207–222. https://doi.org/10.1016/j.jseaes.2005.03.003.

Kieft, R.L., Jackson, C.A.-L., Hampson, G.J., Larsen, E., 2010. Sedimentology and sequence stratigraphy of the hugin formation, quadrant 15, Norwegian sector, south viking graben. Petroleum Geology Conference series 7 (1), 157–176. https://doi.org/10.1144/0070157.

Koskeridou, E., Ioakin, C., 2009. An early Pleistocene mollusc fauna with Ponto-Caspian elements in intra-Hellenic Basin of Atlanti, Arkitsa region (Central Greece). 9th Symposium on Oceanography and Fisheries, pp. 96–101.

Koymans, M.R., Langereis, C.G., Pastor-Galan, D., Hinsbergen, D., 2016. Paleomagnetism.org: an online multi-platform open source environment for paleomagnetic data analysis. Comput. Geosci. 93, 127–137.

Krijgsman, W., Palcu, D.V., Andreetto, F., Stoica, M., Mandic, O., 2020a. Changing seas in the late Miocene northern aegean: a paratethyan approach to mediterranean basin evolution. Earth Sci. Rev. 210, 103386. https://doi.org/10.1016/j.earscirev.2020.103386.

Krijgsman, W., Stoica, M., Hoyle, T.M., Jorissen, E.L., Lazarev, S., Rausch, L., Bista, D., Alçiçek, M.C., Ilgar, A., van den Hoek Ostende, L.W., Mayda, S., Raffi, I., Flecker, R., Mandic, O., Neubauer, T.A., Wesselingh, F.P., 2020b. The myth of the messinian dardanelles: late Miocene stratigraphy and palaeogeography of the ancient aegean-black sea gateway. Palaeogeogr. Palaeoclimatol. Palaeoecol. 560, 110033. https://doi.org/10.1016/j.palaeo.2020.110033.

Krijgsman, W., Tesakov, A., Yanina, T., Lazarev, S., Danukalova, G., van Baak, C., Agustí, J., Alçiçek, M.C., Aliyeva, E., Bista, D., Bruch, A., Büyükmeriç, Y., Bukhsianidze, M., Flecker, R., Frolov, P., Hoyle, T.M., Jorissen, E.L., Kirscher, U., Koriche, S.A., Kroonenberg, S.B., Lordkipanidze, D., Oms, O., Rausch, L., Singarayer, J., Stoica, M., van de Velde, S., Titov, V.V., Wesselingh, F.P., 2019. Quaternary time scales for the Pontocaspian domain: interbasinal connectivity and faunal evolution. Earth Sci. Rev. 188, 1–40. https://doi.org/10.1016/j.earscirev.2018.10.013.

Krstić, N., 1973. Biostratigraphy of the congerian beds in the belgrade region on the basis of ostracoda with the description of the species of the genus amplocypris. Institute for geological and mining explorations and investigation of nuclear and other minerals raw materias. Monographs 4, 208.

Kuiper, K.F., Deino, A., Hilgen, F.J., Krijgsman, W., Renne, P.R., Wijbrans, J.R., 2008. Synchronizing rock clocks of Earth history. Science (New York, N.Y.) 320 (5875), 500–504. https://doi.org/10.1126/science.1154319.

Lazarev, S., 2020. From the Eastern Paratethys to the Pontocaspian Basins: Late Miocene–Middle Pleistocene Magnetobiostratigraphy, Sedimentary Architecture and Faunal Turnovers of the Shrinking Basins of West Eurasia. PhD. Utrecht University, Utrecht.

Lazarev, S., Jorissen, E.L., van de Velde, S., Rausch, L., Stoica, M., Wesselingh, F.P., van Baak, C.G., Yanina, T.A., Aliyeva, E., Krijgsman, W., 2019. Magneto-biostratigraphic age constraints on the palaeoenvironmental evolution of the South Caspian basin during the Early-Middle Pleistocene (Kura basin, Azerbaijan). Quat. Sci. Rev. 222, 105895. https://doi.org/10.1016/j.quascirev.2019.105895.

Lazarev, S., Kuiper, K.F., Oms, O., Bukhsianidze, M., Vasilyan, D., Jorissen, E.L., Bouwmeester, M.J., Aghayeva, V., van Amerongen, A.J., Agustí, J., Lordkipanidze, D., Krijgsman, W., 2021. Five-fold expansion of the Caspian Sea in the late Pliocene: new and revised magnetostratigraphic and 40Ar/39Ar age constraints on the akchagylian stage. Global Planet. Change, 103624. https://doi.org/10.1016/j.gloplacha.2021.103624.

Lazarev, S., Leeuw, A. de, Stoica, M., Mandic, O., van Baak, C., Vasiliev, I., Krijgsman, W., 2020. From khersonian drying to pontian "flooding": late Miocene stratigraphy and palaeoenvironmental evolution of the Dacian Basin (eastern Paratethys). Global Planet. Change 192, 103224. https://doi.org/10.1016/j.gloplacha.2020.103224.

Le Pichon, X., Angelier, J., Sibuet, J., 1982. Plate boundaries and extensional tectonics. Tectonophysics 81 (3–4), 239–256. https://doi.org/10.1016/0040-1951(82)90131-7.

Lee, J.-Y., Marti, K., Severinghaus, J.P., Kawamura, K., Yoo, H.-S., Lee, J.B., Kim, J.S., 2006. A redetermination of the isotopic abundances of atmospheric Ar. Geochem.

Cosmochim. Acta 70 (17), 4507–4512. https://doi.org/10.1016/j.gca.2006.06.1563.

Li, H.-C., Ku, T.-L., 1997. δ13C–δ18C covariance as a paleohydrological indicator for closed-basin lakes. Palaeogeogr. Palaeoclimatol. Palaeoecol. 133 (1–2), 69–80. https://doi.org/10.1016/S0031-0182(96)00153-8.

Lüttig, G.W., Steffens, P., 1975. Paleogeographic Atlas of Turkey 1:1500000 from the Oligocene to the Pleistocene. Scherrerdruck.

Marret, F., Zonneveld, K.A., 2003. Atlas of modern organic-walled dinoflagellate cyst distribution. Rev. Palaeobot. Palynol. 125 (1–2), 1–200. https://doi.org/10.1016/S0034-6667(02)00229-4.

Matoshko, A., Leeuw, A. de, Stoica, M., Mandic, O., Vasiliev, I., Floroiu, A., Krijgsman, W., 2023. The Mio-Pliocene transition in the Dacian Basin (Eastern Paratethys): Paleomagnetism, mollusks, microfauna and sedimentary facies of the Pontian regional stage. Geobios 77, 45–70. https://doi.org/10.1016/j.geobios.2023.03.002.

Matzke-Karasz, R., Witt, W., 2005. Ostracods of the paratethyan Neogene Kilic and yalakdere formations near yalova (İzmit province, Turkey). Zitteliana A45, 111–129.

McArthur, J.M., Howarth, R.J., Shields, G.A., Zhou, Y., 2020. Strontium isotope stratigraphy. In: Geologic Time Scale 2020, pp. 211–238.

McFadden, P.L., McElhinny, M.W., 1990. Classification of the reversal test in palaeomagnetism. Geophys. J. Int. 103 (3), 725–729. https://doi.org/10.1111/j.1365-246X.1990.tb05683.x.

Meijers, M.J., Brocard, G.Y., Whitney, D.L., Mulch, A., 2020. Paleoenvironmental conditions and drainage evolution of the central Anatolian lake system (Turkey) during late Miocene to Pliocene surface uplift. Geosphere 16 (2), 490–509. https://doi.org/10.1130/GES02135.1.

Miall, A.D., 1996. The Geology of Fluvial Deposits: Sedimentary Facies, Basin Analysis, and Petroleum Geology/Andrew D. Miall. Springer, Berlin, London.

Min, K., Mundil, R., Renne, P.R., Ludwig, K.R., 2000. A test for systematic errors in 40Ar/39Ar geochronology through comparison with U/Pb analysis of a 1.1-Ga rhyolite. Geochem. Cosmochim. Acta 64 (1), 73–98.

Mudie, P.J., Aksu, A.E., Yasar, D., 2001. Late Quaternary dinoflagellate cysts from the Black, Marmara and Aegean seas: variations in assemblages, morphology and paleosalinity. Mar. Micropaleontol. 43 (1–2), 155–178. https://doi.org/10.1016/S0377-8398(01)00006-8.

Mudie, P.J., Marret, F., Mertens, K.N., Shumilovskikh, L, Leroy, S.A., 2017. Atlas of modern dinoflagellate cyst distributions in the Black Sea corridor: from aegean to aral seas, including marmara, black, azov and caspian seas. Mar. Micropaleontol. 134, 1–152. https://doi.org/10.1016/j.marmicro.2017.05.004.

Neubauer, T.A., Wesselingh, F.P., 2023. The Early Pleistocene freshwater mollusks of the Denizli Basin (Turkey): a new long-lived lake fauna at the crossroads of Pontocaspian and Aegean-Anatolian realms. ZITT 97, 53–88. https://doi.org/10.3897/zitteliana.97.115682.

Olteanu, R., 1989. La faune d'ostracodes pontiens du Bassin Dacique. Chronostratigraphie und Neostratotypen, Pliozän Pl1, Pontien, pp. 722–752.

Pipík, R., Bodergat, A.-M., 2007. Candoninae trapézoïdales (Crustacea, Ostracoda) du Bassin de Turiec (Slovaquie) du Miocène supérieur systématique, écologie et évolution. Geobios 40 (5), 645–676. https://doi.org/10.1016/j.geobios.2006.02.003.

Popov, S.V., 2004. Lithological-paleogeographic maps of Paratethys: 10 maps late eocene to Pliocene. Courier Forschungsinstitut Senckenberg. E Schweizerbart'sche Verlagsbuchhandlung, Stuttgart.

Raffi, I., Wade, B.S., Pälike, H., Beu, A.G., Cooper, R., Crundwell, M.P., Krijgsman, W., Moore, T., Raine, I., Sardella, R., Vernyhorova, Y.V., 2020. The Neogene period. In: Geologic Time Scale 2020, pp. 1141–1215.

Rausch, L., Stoica, M., Lazarev, S., 2020. A late Miocene - early Pliocene Paratethyan type ostracod fauna from the Denizli Basin (SW Anatolia) and its paleogeographic implications. Acta Palaeontologica Romaniae submitted for publication.

Rochon, A., Mudie, P.J., Aksu, A.E., Gillespie, H., 2002. *Pterocysta* gen. nov.: a new dinoflagellate cyst from pleistocene glacial-stage sediments of the black and Marmara Seas. Palynology 26 (1), 95–105. https://doi.org/10.1080/01916122.2002.9989568.

Sands, A.F., Sereda, S.V., Stelbrink, B., Neubauer, T.A., Lazarev, S., Wilke, T., Albrecht, C., 2019. Contributions of biogeographical functions to species accumulation may change over time in refugial regions. J. Biogeogr. 46 (6), 1274–1286. https://doi.org/10.1111/jbi.13590.

Saraç, G., 2003. Türkiye Omurgalı Fosil Yatakları. Jeoloji Etütleri Dairesi Başkanliği, Ankara.

Sarica, N., 2000. The Plio-Pleistocene age of Byk Menderes and Gediz grabens and their tectonic significance on N-S extensional tectonics in West Anatolia: mammalian evidence from the continental deposits. Geol. J. 35 (1), 1–24. https://doi.org/10.1002/(SICI)1099-1034(200001/03)35:1<1:AID-GJ834>3.0.CO;2-A.

Şengör, A., Yilmaz, Y., 1981. Tethyan evolution of Turkey: a plate tectonic approach. Tectonophysics 75 (3–4), 181–241. https://doi.org/10.1016/0040-1951(81)90275-4.

Shumilovskikh, L.S., Marret, F., Fleitmann, D., Arz, H.W., Nowaczyk, N., Behling, H., 2013. Eemian and Holocene sea-surface conditions in the southern Black Sea: organic-walled dinoflagellate cyst record from core 22-GC3. Mar. Micropaleontol. 101, 146–160. https://doi.org/10.1016/j.marmicro.2013.02.001.

Sickenberg, O., Tobien, H., 1971. New Neogene and lower quaternary vertebrate faunas in Turkey. Newsl. Stratigr. 1 (3), 51–61.

Sokač, A., 1972. Pannonian and Pontian Ostracode fauna of Mt. Medvednica: panonska i pontska fauna ostrakoda Medvednice. Palaeontol. Jugosl. 11, 1–140.

Soliman, A., Riding, J.B., 2017. Late Miocene (tortonian) gonyaulacacean dinoflagellate cysts from the Vienna basin, Austria. Rev. Palaeobot. Palynol. 244, 325–346. https://doi.org/10.1016/j.revpalbo.2017.02.003.

Spötl, C., Vennemann, T.W., 2003. Continuous-flow isotope ratio mass spectrometric analysis of carbonate minerals. Rapid communications in mass spectrometry RCM 17 (9), 1004–1006. https://doi.org/10.1002/rcm.1010.

Stoica, M., Lazăr, I., Krijgsman, W., Vasiliev, I., Jipa, D., Floroiu, A., 2013. Paleoenvironmental evolution of the East carpathian foredeep during the late miocene–early Pliocene (Dacian Basin; Romania). Global Planet. Change 103, 135–148. https://doi.org/10.1016/j.gloplacha.2012.04.004.

Sümer, Ö., İnci, U., Sözbilir, H., 2012. Tectono-sedimentary evolution of an Early Pleistocene shallow marine fan-deltaic succession at the western coast of Turkey. Geodinamica Acta 25 (3–4), 112–131. https://doi.org/10.1080/09853111.2013.877241.

Sun, S., 1990. Denizli-Uşak Arasinin Jeolojisi Ve Linyit Olanaklari, vol. 9985. MTA Raporu (In Turkish).

Sütö-Szentai, M., 1982. A Tengelic-2. sz. fúrás pannóniai képződményeinek szervesvázú mikroplankton és sporomorpha maradványai. Annales Instituti Geologici Publici Hungarici 65.

Sütö-Szentai, M., 2010. Definition and description of new dinoflagellate genus, species and subspecies from the Pannonian Stage (Hungary). Acta Naturalia Pannonica 1 (2), 223–239.

Sütö-Szentai, M., 2000. Organic walled microplankton zonation of the pannonian S.L. In the surroundings of the kaskantyú, paks and tengelic (Hungary). Annual Report of the Geological Institute of Hungary. 1994–1995 (II), 153–175.

Tauxe, L., Kent, D.V., 2004. A simplified statistical model for the geomagnetic field and the detection of shallow bias in paleomagnetic inclinations: was the ancient magnetic field dipolar? In: Channell, J., Kent, D.V., Lowrie, W., Meert, J.G. (Eds.), Timescales of the Paleomagnetic Field. American Geophysical Union, Washington, D. C., pp. 101–115

Ten Veen, J.H., Boulton, S.J., Alçiçek, M.C., 2009. From palaeotectonics to neotectonics in the Neotethys realm: the importance of kinematic decoupling and inherited structural grain in SW Anatolia (Turkey). Tectonophysics 473 (1–2), 261–281. https://doi.org/10.1016/j.tecto.2008.09.030.

Tunoglu, C., Ünal, A., 2001. Pannonian-pontian ostracod fauna of gelibolu Neogene basin (NW Turkey). Yerbilimleri 23, 167–187.

Tunoğlu, C., 2003. Systematics and biostratigraphy of the pontian candonidae (ostracoda) from the eastern Black Sea region (northern Turkey). Geologica carpathica-Bratislava 54 (1), 21–40.

Uzel, B., Sozbilir, H., Ozkaymak, C., 2012. Neotectonic evolution of an actively growing superimposed Basin in western Anatolia: the inner Bay of izmir, Turkey. Turk. J. Earth Sci. https://doi.org/10.3906/yer-0910-11.

van Baak, C., Grothe, A., Richards, K., Stoica, M., Aliyeva, E., Davies, G., Kuiper, K.F., Krijgsman, W., 2019. Flooding of the Caspian Sea at the intensification of northern hemisphere glaciations. Global Planet. Change 174, 153–163. https://doi.org/10.1016/j.gloplacha.2019.01.007.

van Baak, C., Vasiliev, I., Stoica, M., Kuiper, K.F., Forte, A.M., Aliyeva, E., Krijgsman, W., 2013. A magnetostratigraphic time frame for Plio-Pleistocene transgressions in the South Caspian Basin, Azerbaijan. Global Planet. Change 103, 119–134. https://doi.org/10.1016/j.gloplacha.2012.05.004.

van Baak, C.G., Mandic, O., Lazar, I., Stoica, M., Krijgsman, W., 2015. The Slanicul de Buzau section, a unit stratotype for the Romanian stage of the Dacian Basin (Plio-Pleistocene, Eastern Paratethys). Palaeogeogr. Palaeoclimatol. Palaeoecol. 440, 594–613. https://doi.org/10.1016/j.palaeo.2015.09.022.

Vekua, M.K., 1975. The Ostracods of the Kimmerian and Kujalinikian Deposits of Abkhazia and Their Stratigraphic Significance. Metsniereba, Tbilisi.

Wall, D., Dale, B., Harada, K., 1973. Descriptions of new fossil dinoflagellates from the late quaternary of the Black Sea. Micropaleontology 19 (1), 18. https://doi.org/10.2307/1484962.

Wesselingh, F.P., Alçiçek, H., 2010. A new cardiid bivalve from the Pliocene Baklan Basin (Turkey) and the origin of modern Ponto-Caspian taxa. Palaeontology 53 (4), 711–719. https://doi.org/10.1111/j.1475-4983.2010.00958.x.

Wesselingh, F.P., Alçiçek, H., Magyar, I., 2008. A Late Miocene Paratethyan mollusc fauna from the Denizli Basin (southwestern Anatolia, Turkey) and its regional palaeobiogeographic implications. Geobios 41 (6), 861–879. https://doi.org/10.1016/j.geobios.2008.07.003.

Wilke, T., Albrecht, C., Anistratenko, V.V., Sahin, S.K., Yildirim, M.Z., 2007. Testing biogeographical hypotheses in space and time: faunal relationships of the putative ancient Lake Eg?irdir in Asia Minor. J. Biogeogr. 34 (10), 1807–1821. https://doi.org/10.1111/j.1365-2699.2007.01727.x.

Yalçınlar, I., 1983. Türkiye'de Neojen ve Kuvaterner omurgalı arazileri ve jeomorfolojik karakterleri [Neogene and Quaternary Vertebrate Fields of Turkey and their Geomorphologic Characteristics]. Publication of Faculty of Literature, Istanbul.

Zonneveld, K.A., Marret, F., Versteegh, G.J., Bogus, K., Bonnet, S., Bouimetarhan, I., Crouch, E., Vernal, A. de, Elshanawany, R., Edwards, L., Esper, O., Forke, S., Grøsfjeld, K., Henry, M., Holzwarth, U., Kielt, J.-F., Kim, S.-Y., Ladouceur, S., Ledu, D., Chen, L., Limoges, A., Londeix, L., Lu, S.-H., Mahmoud, M.S., Marino, G., Matsouka, K., Matthiessen, J., Mildenhal, D.C., Mudie, P., Neil, H.L., Pospelova, V., Qi, Y., Radi, T., Richerol, T., Rochon, A., Sangiorgi, F., Solignac, S., Turon, J.-L., Verleye, T., Wang, Y., Wang, Z., Young, M., 2013. Atlas of modern dinoflagellate cyst distribution based on 2405 data points. Rev. Palaeobot. Palynol. 191, 1–197. https://doi.org/10.1016/j.revpalbo.2012.08.003.